

Robust Output Regulation for Nonlinear Chemical Processes with Unmeasurable Disturbances

Wei Wu and Yi-Shyong Chou

Dept. of Chemical Engineering, National Taiwan Institute of Technology, Taipei 10672, Taiwan, ROC

It becomes a problem when the input-output feedback linearization of nonlinear processes presents unmeasurable disturbances that appear linear in the model and are not in the span of control input space. The presented hybrid nonlinear controller, which consists of a nonlinear static state feedback with a series of adjustable parameters and an internal model, can achieve disturbance attenuation and offset-free performance. The major advantage of the proposed control system design is to reject disturbance without producing a vigorous control action. A simple estimation method of computing a single parameter that replaces a series of adjustable parameters of the controller is developed. The proposed estimation strategy of computing a single parameter is based on the Lyapunov stability theory. These control schemes are illustrated by an example of a chemical reactor to obtain satisfactory control.

Introduction

Recent developments in the theory of differential geometry provide useful methods for a class of nonlinear systems. The central concept of this approach is to algebraically transform the nonlinear system into the equivalent linear system, such that conventional linear control techniques can also be applied (Isidori, 1989; Nijmeijer and van der Schaft, 1990). Assuming that system states are available, in these new coordinates the transformed system can exhibit linear dynamics. Generally, the nonlinear geometric control technique requires the accurate mathematical model of the plant to achieve exact cancellation of nonlinear terms. But this cancellation is no longer exact when there exist unmeasurable disturbances or modeling errors. Therefore, the design of a robust stabilizing controller that deals with nonlinear systems in the presence of unmeasurable disturbances and uncertainties is an important subject for design of a satisfactory and efficient control system.

Despite the significant progress and the growing interest in nonlinear geometric control, existing equivalent classes and output tracking design techniques rarely address the nonlinear systems in the presence of unmeasurable disturbances and uncertainties. In the design of an output regulation of chemical processes, a proportional-integral (PI) controller (Kravaris and Chung, 1987) or an internal model control (IMC) (Calvet

and Arkun, 1988) is usually implemented in the outer loop of nonlinear geometric control design to attenuate the effects of unmeasurable disturbances or unmodeling dynamics on the system output. Calvet and Arkun (1990) and Arkun and Calvet (1992) have proposed a P or PI stabilizing controller based on an algebraic Riccati equation to ensure closed-loop system stability in the presence of parametric uncertainty. Henson and Seborg (1991) have developed a new methodology to derive a nonlinear controller based on the IMC framework and have suggested incorporating a nonlinear filter for achieving robustness. Shukla et al. (1992) have proposed a nonlinear controller using the IMC framework and have shown its capability for controlling a nonlinear pH process.

To reduce as much as possible the influence of external disturbances and uncertainties on the tracking error or regulated output responses, a high-gain control design is usually used to achieve this purpose. In the implementation of such control laws, undesirable effects like high control activity and controller saturation may result in the controller being easily worn down and the closed-loop system being unstable. In particular, for most chemical processes containing the unmodeled high-frequency noises and the constrained control behaviors, this approach is no longer suitable. In this article, we study the output tracking problem in the presence of unmeasurable disturbances that do not satisfy the so-called matching condition and avoid employing the conventional

Correspondence concerning this article should be addressed to Y.-S. Chou.

high-gain control design. The proposed *hybrid* nonlinear control is a combination of a set of adjustable parameters and an internal model to compensate beforehand for the effects of unmeasurable disturbances on the system output. Therefore, the robustness and performance of the controlled system can be improved. A useful estimation method of a single parameter that replaces a series of adjustable parameters of the proposed hybrid controller is developed. Here we analyze the presented estimation method by the Lyapunov stability theory and make sure that it is feasible and practical. Finally, the proposed control schemes are evaluated through an example of a continuous stirred tank reactor (CSTR).

Problem Formulation and Analysis

The purpose of the synthesis methodology to be presented is to provide a systematic control framework for a class of single-input single-output (SISO) nonlinear systems forced by exogenous input disturbances that are bounded and smooth. More precisely, we will consider a class of nonlinear systems with a state-space representation of the form:

$$\begin{aligned}\dot{x} &= f(x) + g(x)u + \sum_{i=1}^m \omega_i(x, u) d_i(t) \\ y &= h(x),\end{aligned}\quad (1)$$

where $f(x)$, $g(x)$, and $\omega_i(x, u)$, $i = 1, 2, \dots, m$, are known vector fields on \mathbb{R}^n ; x is an n -dimensional state vector; u is a scalar manipulated input; y is a scalar controlled output; $h(x)$ is a scalar output function; and $d_i \in \mathbb{R}$, $i = 1, 2, \dots, m$, are unmeasurable disturbances. It is assumed that a specified time-varying function d_i has the property:

$$\exists t^* > 0 \text{ s.t. } d_i(t) = \text{constant } d_i^{ss}, \quad i = 1, 2, \dots, m, \quad \forall t > t^* \quad (2)$$

within a prescribed compact set $\Sigma \subset \mathbb{R}^m$, and d_i^{ss} is a fixed but unknown constant. Here we restrict ourselves to consider a class of SISO nonlinear systems in the presence of disturbances that appear linear in the model. Although such a consideration cannot handle all disturbances, the proposed method will provide the new solution of this class of nonlinear systems. Calvet and Arkun (1988), Daoutidis and Kravaris (1989), and Poslavsky and Kantor (1991) have investigated a similar problem, like Eq. 1.

The corresponding system without external disturbances, which satisfies the desired operating point x^d and u^d , is expressed as

$$f(x^d) + g(x^d)u^d = 0. \quad (3)$$

Furthermore, the important property of the input-output linearization theory is its relative degree (Isidori, 1989). In essence, the relative degree represents the number of times the output y must be differentiated with respect to time until the effect of input appears. The relative degree r of the manipulated input and relative degree \tilde{r}_i of the disturbance d_i are defined as

$$r \equiv \min\{k: L_g L_f^{k-1} h(x) \neq 0\} \quad (4)$$

$$\tilde{r}_i \equiv \min\{k: L_{\omega_i} L_f^{k-1} h(x) \neq 0\}, \quad i = 1, 2, \dots, m. \quad (5)$$

To compare the relative effects of the manipulated input and the disturbances on the output, the disturbances can be categorized as follows:

$$D_A \equiv \{d_i(t): \tilde{r}_i > r, \quad i = 1, 2, \dots, m\} \quad (6)$$

$$D_B \equiv \{d_i(t): \tilde{r}_i \leq r, \quad i = 1, 2, \dots, m\}. \quad (7)$$

Since they affect the output less directly than the manipulated input, the D_A disturbances can be decoupled from the output with a static state feedback control. The D_B disturbances affect the output more directly than the input and, therefore, may be almost decoupled by a high-gain feedback technique with the singular perturbation approach (Marino et al., 1989). But this approach is not considered here.

Design model

To investigate control design in this article we assume that the disturbance relative degree belongs to the set of D_B . Usually unmeasurable disturbances cannot be directly handled by the feedforward control strategy. Therefore, we will consider the following design model, which incorporates a series of known constants as follows:

$$\dot{x} = f_d[x, p^*(t), u] + g(x)u \quad (8)$$

with

$$f_d[x, p^*(t), u] = f(x) + \sum_{i=1}^m \omega_i(x, u) p_i^*(t), \quad x(0) = x^d, \quad (9)$$

where $p^* = [p_1^*, p_2^*, \dots, p_m^*]^T$ is the known and piecewise constant vector as tuning parameters on a bounded set $\Pi \subset \Sigma \in \mathbb{R}^m$, that is,

$$\exists t_0, t_1 > 0 \quad \text{s.t.} \quad p_i^*(t) = \text{constant } p_i, \quad i = 1, 2, \dots, m, \quad \forall t \in [t_0, t_1]. \quad (10)$$

The class of design model we shall deal with is characterized by the following assumption.

Assumption 1. Consider the design model (Eq. 8) and the controlled output (Eq. 1) for every $x \in \mathbb{R}^n$ and $p^* \in \Pi$:

- A uniform relative degree r , that is,

$$(L_g h)(x) = \dots = (L_g L_f^{r-2} h)(x, p^*) = 0, \quad (11)$$

$$(L_g L_f^{r-1} h)(x, p^*) \neq 0. \quad (12)$$

- The mapping $(\xi, \eta) = T(x, p^*)$, defined by

$$\xi_i = T_i(x, p^*) = (L_{f_d}^{i-1} h)(x, p^*), \quad i = 1, 2, \dots, r \quad (13)$$

and

$$\eta_j = T_i(x, p^*), \quad i = r+1, r+2, \dots, n \quad \text{and} \quad j = 1, 2, \dots, n-r, \quad (14)$$

satisfying

$$L_g \eta_j = 0, \quad j = 1, 2, \dots, n-r, \quad (15)$$

where the symbol $(\cdot)(x, p^*)$ represents the nonlinear operator, which is a function of the variable x and the parameter p^* .

It is well known (Isidori, 1989; Khalil and Esfandiari, 1993) that the assumption of uniform relative degree is a necessary and sufficient condition for the mapping $(\xi, \eta) = T(x, p^*)$ to be a local diffeomorphism in the neighborhood of every $x \in \mathbb{R}^n$ and $p^* \in \Pi$. Under assumption 1, in Eq. 8 we consider the output $y = \xi_1$ and its derivatives shown as

$$\begin{aligned} \dot{\xi}_1 &= (L_{f_d} h)(x, p^*) + u(L_g h)(x) = \xi_2 \\ \dot{\xi}_2 &= (L_{f_d}^2 h)(x, p^*) + u(L_g L_{f_d} h)(x, p^*) + \sum_{i=1}^m \frac{\partial (L_{f_d} h)}{\partial p_i^*} \dot{p}_i^* \\ &= \xi_3 + (L_{\dot{p}} L_{f_d} h)(x, p^*, \dot{p}^*) \\ &\vdots \\ \dot{\xi}_r &= (L_{f_d}^r h)(x, p^*, u) + u(L_g L_{f_d}^{r-1} h)(x, p^*) + \sum_{i=1}^m \frac{\partial (L_{f_d}^{r-1} h)}{\partial p_i^*} \dot{p}_i^* \\ \dot{\eta}_j &= (L_{f_d} \eta_j)(x, p^*) + u(L_g \eta_j)(x, p^*) + \sum_{i=1}^m \frac{\partial (L_{f_d} \eta_j)}{\partial p_i^*} \dot{p}_i^* \\ &= (L_{f_d} \eta_j)(x, p^*) + (L_{\dot{p}} L_{f_d} \eta_j)(x, p^*, \dot{p}^*), \quad j = 1, 2, \dots, n-r. \end{aligned} \quad (16)$$

Under the previous conditions (Eq. 10), we can consider $\dot{p}^* = 0$ and $p^* = p$ during a time period. Hence the change of variables $(\xi, \eta) = T(x, p)$, for every $t \in [t_0, t_1]$, transforms Eq. 16 into the normal form

$$\begin{aligned} \dot{\xi}_1 &= \xi_2 \\ &\vdots \\ \dot{\xi}_{r-1} &= \xi_r \\ \dot{\xi}_r &= (L_{f_d} h)(x, p, u) + u(L_g L_{f_d}^{r-1} h)(x, p) \\ \dot{\eta} &= q(\xi, \eta) \\ y &= \xi_1, \end{aligned} \quad (17)$$

where $q(\cdot) \in \mathbb{R}^{n-r}$ is a nonlinear function and $q(\xi, \eta) = (d\eta \circ f_d) \circ T^{-1}(\xi, \eta)$. Notice that the symbol \circ denotes a composition function operator.

Moreover, if the nonlinear algebraic equation,

$$(L_{f_d}^r h)(x, p, u) + u(L_g L_{f_d}^{r-1} h)(x, p) = v, \quad \forall t \in [t_0, t_1] \quad (18)$$

can be solved for u , then it follows from Eq. 17 that the map from the new input v to the output is linearized:

$$y^{(r)} = v, \quad \forall t \in [t_0, t_1]. \quad (19)$$

According to the implicit function theorem (Nijmeijer and van der Schaft, 1990), there exists a parameterized static state feedback control law:

$$u = \gamma_0(x, p, v), \quad \forall t \in [t_0, t_1] \quad (20)$$

that is the solution of Eq. 18. It is shown that there exists a u_s for every x_s , p_s , and v_s such that:

$$(L_{f_d}^r h)(x_s, p_s, u_s) + u_s(L_g L_{f_d}^{r-1} h)(x_s, p_s) = v_s, \quad \forall t \in [t_0, t_1] \quad (21)$$

is satisfied. In general, the control law (Eq. 20) can be obtained in the numerical form from Eq. 18. It is important to note that the singular points in the control law must be carefully avoided. Indeed, the control law (Eq. 20) is a feedforward/state feedback controller if d_i is measurable and $p_i = d_i^{ss}$ (Calvet and Arkun, 1988; Daoutidis and Kravaris, 1989; Henson and Seborg, 1990). Thus, the solution to Eq. 20 has "feedforward-like" characteristics.

Minimum phase system

The control law (Eq. 20) also makes the state vector η completely unobservable at the output. However, we observe that ξ can be thought of as an external input vector with respect to the dynamics of η . The dynamics:

$$\dot{\eta} = q(0, \eta) \quad (22)$$

are referred to as the zero dynamics. Systems in which the zero dynamics are asymptotically stable are called the minimum-phase system. For the purposes of stable tracking, we require that the stronger stability criteria for the dynamics:

$$\dot{\eta} = q(\xi, \eta) \quad (23)$$

be bounded-input bounded-state (BIBS) stable. If the design model has the BIBS property, we say that the model has stable inverse (Henson and Seborg, 1991; Sussman and Kokotovic, 1991). We will use the following assumption regarding the minimum-phase condition throughout this article.

Assumption 2. The zero dynamics (Eq. 22) is exponentially stable in its domain of definition. Moreover, the function $q(\xi, \eta)$ is Lipschitz in ξ , uniformly in η .

By the converse theorem of Lyapunov (Khalil, 1992), the exponential stability property of the zero dynamics induces a Lyapunov function $W_0(\eta)$ that satisfies the following inequalities:

$$\begin{aligned}
k_1 \|\eta\|^2 &\leq W_0(\eta) \leq k_2 \|\eta\|^2 \\
\frac{\partial W_0}{\partial \eta} q(0, \eta) &\leq -k_3 \|\eta\|^2 \\
\left\| \frac{\partial W_0}{\partial \eta} \right\| &\leq k_4 \|\eta\|
\end{aligned} \quad (24)$$

for some positive constants k_1 , k_2 , k_3 , and k_4 .

Since $q(\xi, \eta)$ is Lipschitz in ξ (Khalilk, 1992), there exists a positive constant L such that:

$$\|q(\xi, \eta) - q(0, \eta)\| \leq L \|\xi\|, \quad (25)$$

where L is called a Lipschitz constant of $q(\xi, \eta)$.

We are now ready to design a *hybrid* nonlinear controller based on the design model (Eq. 8) and an internal linear model to be implemented for a class of nonlinear systems for the purpose of disturbance attenuation. These detailed formulations and properties are introduced in the following section.

Hybrid Nonlinear Control

In this section, the hybrid nonlinear control that is given can simultaneously overcome the problem of unmeasurable disturbances that do not satisfy the matching condition, that is, it belongs to the set of D_B in Eq. 7, and the problem of the system trajectory asymptotically tracking the desired setpoint.

Let us consider the plant (Eq. 1) based on the design model (Eq. 8) for every $t \in [t_0, t_1]$, such that it can be represented as:

$$\begin{aligned}
\dot{x} &= f(x) + \sum_{i=1}^m \omega_i(x, u) p_i + g(x)u + \sum_{i=1}^m \omega_i(x, u) d_i(t) \\
&\quad - \sum_{i=1}^m \omega_i(x, u) p_i \\
&= f_d(x, p, u) + g(x)u + \sum_{i=1}^m [d_i(t) - p_i] \omega_i(x, u) \\
y &= h(x).
\end{aligned} \quad (26)$$

Under assumption 1, and using the input-output feedback linearization algorithm, yields:

$$\begin{aligned}
\dot{\xi}_1 &= \xi_2 + \sum_{i=1}^m [d_i(t) - p_i] \Delta A_{i1}(x, u) \\
&\vdots \\
\dot{\xi}_{r-1} &= \xi_r + \sum_{i=1}^m [d_i(t) - p_i] \Delta A_{i, r-1}(x, p, u) \\
\dot{\xi}_r &= (L_{f_d}^r h)(x, p, u) + u (L_g L_{f_d}^{r-1} h)(x, p) \\
&\quad + \sum_{i=1}^m [d_i(t) - p_i] (L_{\omega_i} L_{f_d}^{r-1} h)(x, p, u)
\end{aligned}$$

$$\begin{aligned}
&= v + \sum_{i=1}^m [d_i(t) - p_i] \Delta A_{i_r}(x, u) \\
\dot{\eta}_j &= q_j(\xi, \eta) + \sum_{i=1}^m [d_i(t) - p_i] \Delta \phi_{ij}(x, p, u), \\
&\quad j = 1, 2, \dots, n-r \\
y &= \xi_1
\end{aligned} \quad (27)$$

In the process control problem, the output y is usually required to asymptotically track a setpoint, y_{sp} , that is, $\lim_{t \rightarrow \infty} y(t) = y_{sp}$. At the present time the model-based control has become a popular and practical control design. In particular, the IMC is frequently used to improve the system robustness and performance (Morari and Zafiriou, 1989; Henson and Seborg, 1991; Shukla et al., 1992). Here the new *hybrid* nonlinear controller containing an internal linear model will be presented as follows.

First, the specified linear controllable model is described as:

$$\begin{aligned}
\dot{z} &= A_0 z + B_0 v_d \\
y_m &= C_0 z,
\end{aligned} \quad (28)$$

where z is an r -dimensional state vector; A_0 is an $r \times r$ matrix, B_0 is an $r \times 1$ column vector, and C_0 is a $1 \times r$ row vector; v_d is the model control input; and y_m is the controlled output. This is an r -dimensional linear dynamics and the (A_0, B_0) satisfies the controllability conditions (Callier and Desoer, 1991).

Second, this model (Eq. 28) will be used as an internal model for the design of a hybrid controller, for which the following assumption is needed.

Assumption 3. Consider that an internal model (Eq. 28) has the BIBS property, that is, the output y_m and its r derivatives are uniformly bounded for a bounded value B_d ,

$$\|(y_m, y_m^{(1)}, \dots, y_m^{(r)})\| \leq B_d. \quad (29)$$

If the relative degree of the internal model is set as r , and the control input v_d can be designed as an error feedback compensator:

$$v_d = \frac{\epsilon^{-r}}{C_0 A_0^{r-1} B_0} \left[\alpha_1 \delta - \epsilon^r C_0 A_0^r z - \sum_{i=1}^r \alpha_i \epsilon^{i-1} C_0 A_0^{i-1} z \right], \quad (30)$$

where $\epsilon > 0$ is a tuning parameter, $\delta \in \Re$ is denoted as an error feedback signal, and the tuning parameters α_i should be chosen such that:

$$s^r + \alpha_r s^{r-1} + \dots + \alpha_1 \quad (31)$$

is a Hurwitz polynomial where s is a Laplace operator. Such the model in Eq. 28 can be formulated in the following form:

$$\begin{aligned}\epsilon \dot{\xi}_d &= A_c \xi_d + B \alpha_1 \delta \\ y_m &= \xi_{d_1}\end{aligned}\quad (32)$$

where $\xi_{d_i} = \epsilon^{i-1} C_0 A_0^{i-1} z = \epsilon^{i-1} y_m^{(i-1)}$, $i = 1, 2, \dots, r$, and A_c is a Hurwitz matrix shown as

$$A_c = \begin{bmatrix} 0 & 1 & 0 & \cdots & 0 \\ 0 & 0 & 1 & \cdots & 0 \\ \vdots & \vdots & \vdots & \ddots & \vdots \\ 0 & 0 & 0 & 0 & 1 \\ -\alpha_1 & \cdot & \cdot & \cdot & -\alpha_r \end{bmatrix}. \quad (33)$$

Moreover, we can select a symmetric positive definite matrix P_s to satisfy the following Lyapunov equation:

$$A_c^T P_s + P_s A_c = -I \quad (34)$$

where I is an identity matrix. Based on this design, there are two important properties to be investigated as follows.

Regulation

• Selecting $\delta = y_{sp} - y + y_m$ and a sufficiently small value of ϵ in Eq. 30 is equivalent to the high-gain feedback control, that is, Eq. 32 can be reduced to

$$\xi_{d_2} \approx \xi_{d_3} \approx \cdots \approx \xi_{d_r} \approx 0, \quad (35)$$

and $y_m \approx \delta$. Then we obtain

$$y(t) \approx y_{sp}, \quad \forall t > 0 \quad \text{and} \quad \lim_{t \rightarrow \infty} y = y_{sp}. \quad (36)$$

• Choosing the unified parameters in pole placement design, that is,

$$\alpha_{r-j} = \frac{r(r-1)\cdots(r-j)}{(j+1)!} (\alpha_1)^{\frac{j+1}{r}}, \quad j = 0, 1, \dots, r-1. \quad (37)$$

the transfer function of Eq. 32 is then summarized as

$$\frac{y_m}{\delta} = \frac{1}{\left[\epsilon (\alpha_1)^{-1/r} s + 1 \right]^r}. \quad (38)$$

In particular, this case $\alpha_1 = 1$ in Eq. 38 is equivalent to that of the IMC strategy that was introduced by Henson and Seborg (1991). Certainly, the control law in Eq. 30 possesses the IMC properties of good output regulation and no offset performance. Notice that from Eq. 36 the controlled system has an excellent output regulation when the small value of ϵ is used. This situation can cause the actuator to have a vigorous control action in the feedback loop because the smallness of ϵ makes the control input ν_d large, as seen from Eq. 30. If the unified parameters in Eq. 37 are chosen, then the selection of parameters of the Hurwitz polynomial in Eq. 31 can be reduced to adjust the single parameter α_1 . Adjusting α_1 and ϵ is equivalent to adjusting the speed of the system response.

Stability

• Selecting a quadratic function, $V_m = \epsilon \xi_d^T P_s \xi_d$ and with the aid of Eq. 34, the time derivative of the quadratic function along the trajectory of Eq. 32 can be written as:

$$\begin{aligned}\dot{V}_m &= -\|\xi_d\|^2 + \|2\alpha_1 \delta B^T P_s \xi_d\| \\ &\leq -\frac{3}{4} \|\xi_d\|^2 - \left(\frac{\|\xi_d\|^2}{2} - \|2\alpha_1 \delta B^T P_s\| \right)^2 + \|2\alpha_1 \delta B^T P_s\|^2 \\ &\leq -\frac{3}{4} \|\xi_d\|^2 + \|2\alpha_1 \delta B^T P_s\|^2. \quad (39)\end{aligned}$$

If $\dot{V}_m \leq 0$, we obtain

$$|\delta| \leq \frac{\sqrt{3} \|\xi_d\|}{4\alpha_1 \|B^T P_s\|}.$$

It is shown that a model-based control strategy can account for disturbances and nonmodeling errors and leads to the state trajectory within a guaranteed precision. But a large modeling error (a large δ) or rapid decaying ξ_d (i.e., a sufficiently small ϵ) may induce the “peaking” phenomenon and destroy closed-loop stability as shown in Eq. 39.

In this article, our philosophy of control design is that we avoid employing the high-gain control to attenuate input disturbances. We use the feedforward-like compensator to minimize the plant/model mismatch, which is the error between the controlled output y and the linear model output y_m , to achieve cancellation of the disturbance as completely as possible *a priori*. Therefore, the objective of this article is to construct a hybrid nonlinear controller that combines the feedback linearizing control (Eq. 20) for the inner-loop structure as a feedforward-like compensator to provide corrective action, and the model-based control (Eq. 30) for the outer-loop structure as a robust compensator to pursue the superb output trajectory.

To establish the complete control structure, we need to define the trajectory error $e \in \Re^r$ between the linearized system (Eq. 27) and the transformed internal linear model (Eq. 32) as a new coordinate transformation, that is,

$$e_i = \xi_i - y_m^{(i-1)}, \quad i = 1, 2, \dots, r. \quad (40)$$

Then, Eq. 27 can be further expressed as

$$\begin{aligned}\dot{e} &= Ae + B(\nu - y_m^{(r)}) + \sum_{i=1}^m [d_i(t) - p_i] \Delta A_i(x, p, u) \\ \dot{\eta} &= q(\xi, \eta) + \sum_{i=1}^m [d_i(t) - p_i] \Delta \phi_i(x, p, u) \\ e_1 &= y - y_m\end{aligned}\quad (41)$$

where $\Delta A_i = [\Delta A_{i1}, \Delta A_{i2}, \dots, \Delta A_{ir}]^T = [L_{\omega_i} h, L_{\omega_i} L_{f_d} h, \dots, L_{\omega_i} L_{f_d}^{r-1} h]^T$ is an $r \times 1$ column vector, $\Delta \phi_i = [\Delta \phi_{i1}, \Delta \phi_{i2}, \dots, \Delta \phi_{i_{n-r}}]^T = [L_{\omega_i} \eta_1, L_{\omega_i} \eta_2, \dots, L_{\omega_i} \eta_{n-r}]^T$ is an $(n-r) \times 1$ column vector for every $i = 1, 2, \dots, m$; (A , B , C) are in Brunovsky canonical form.

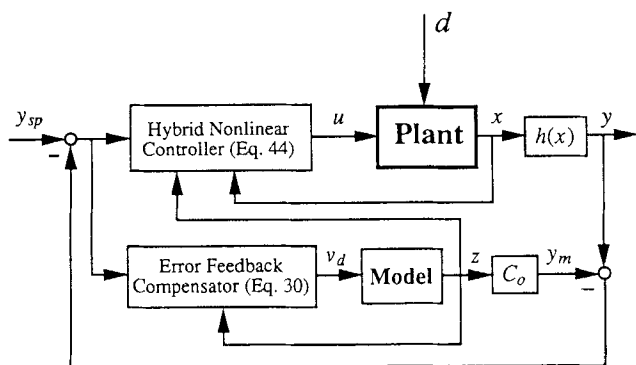


Figure 1. Structure of the hybrid nonlinear control.

Hence, the external control input ν is selected as

$$\nu = C_0 A_0^r z + C_0 A_0^{r-1} B_0 \nu_d + \sum_{i=1}^r \alpha_i (C_0 A_0^{i-1} z - \xi_i). \quad (42)$$

The closed-loop of the regular perturbation system of Eq. 41 for every $t \in [t_0, t_1]$ can be further constructed as follows:

$$\begin{aligned} \dot{e} &= A_c e + \sum_{i=1}^m [d_i(t) - p_i] \Delta A_i(x, p, u) \\ \dot{\eta} &= q(\xi, \eta) + \sum_{i=1}^m [d_i(t) - p_i] \Delta \phi_i(x, p, u) \\ e_1 &= C e. \end{aligned} \quad (43)$$

Combining the previous design Eqs. 20, 30, 37, and 42, the hybrid nonlinear controller can be summarized as

$$\begin{aligned} u &= \gamma_0(x, p, \nu) \\ \nu &= \epsilon^{-r} \alpha_1 (y_{sp} - y + y_m) \\ &+ \sum_{j=0}^{r-1} \frac{r(r-1) \cdots (r-j)}{(j+1)!} (\alpha_1)^{\frac{r-j-1}{r}} \\ &\times \left[(1 - \epsilon^{-(j+1)}) C_0 A_0^{r-j-1} z - \xi_{r-j} \right]. \end{aligned} \quad (44)$$

The detailed structure of the hybrid controller is shown in Figure 1.

It is important to note that the control law presented here consists chiefly of three different parameters p , α_1 , and ϵ . The features of these parameters are addressed as follows. The function of p is that the nonlinearity cancellation in Eq. 43 can be obtained when the parameter p agrees exactly with unmeasurable disturbance d^{ss} after a finite time. In the next section, we will offer an estimation method of a single parameter p_i , $i = 1$, or $i = 2, \dots$, or $i = m$, which replaces a series of tuning parameters of the given control law. Instead of a series of parameters p of the given control law, an appropriately chosen value of p_i can compensate for the effects of unmeasurable disturbances on the system output. The smaller the ϵ or the larger the α_1 we choose, the better the output regulation we have. But the case where the chosen

value of ϵ is too small (i.e., $\epsilon < 1$) or the chosen value of α_1 is too large (i.e., $\alpha_1 > 1$) gives the control loop a vigorous control action, should be avoided.

Stability Analysis and Controller Parameter Tuning

In fact, how to obtain an *exact* nonlinearity cancellation, that is, make the parameter $p^*(t)$ equally match the unmeasurable disturbance $d(t)$ within a finite time, is an important and a very difficult task. However, using the available information, we focus our attention on improving the output regulation, the output tracking error $e_1 = y - y_m$, from the internal model control scheme, as shown in Figure 1, and to design an estimation method for computing an appropriate single parameter p_i , $i = 1$, or $i = 2$, or $i = m$. Such a control design will asymptotically cancel the nonlinearity without offset in the output response. In this section, we will first investigate robust stability conditions and performance results for the regular perturbation system (Eq. 43). Second, we will provide a simple procedure of computing a single controller parameter. Their proofs will be presented in the Appendix.

Lyapunov stability analysis

Here we use the approach of the indirect Lyapunov function to establish the robust stability conditions and performance results. Before this becomes possible, knowledge of nonlinearity is required *a priori*. This is stated in the following assumption.

Assumption 4. The system described in Eq. 44 satisfies the BIBS condition. There exist some suitable positive constants γ_{1i} , γ_{2i} , γ_{3i} , l_{1i} , l_{2i} and l_{3i} , for every $i = 1, 2, \dots, m$ and $t \in [t_0, t_1]$, such that

$$\|2P_s \Delta A_i(x, p, u) \circ T^{-1}(\xi, \eta)\| \leq \gamma_{1i} \|\xi\| + \gamma_{2i} \|\eta\| + \gamma_{3i} \quad (45)$$

$$\|\Delta \phi_i(x, p, u) \circ T^{-1}(\xi, \eta)\| \leq l_{1i} \|\xi\| + l_{2i} \|\eta\| + l_{3i} \quad (46)$$

for every $x \in \mathfrak{R}^n$, and $p \in \Pi$. Moreover, P_s satisfies the Lyapunov equation (Eq. 34).

Notice that these nonlinearities are considered to be non-vanishing in the desired operating point, that is,

$$\Delta A_i(x^d, p, u^d) \neq 0 \quad \text{or} \quad \Delta \phi_i(x^d, p, u^d) \neq 0. \quad (47)$$

The proposed hybrid nonlinear controller will tolerate a class of perturbations (Eq. 43) to some extent to still achieve an overall system stability and to maintain some degree of output tracking performance. Hence, these properties are summarized in the following theorem.

Theorem 1. Assume that the plant in Eq. 1 satisfies assumptions 1–4. There then exist $\mu \leq \max(\mu_1^*, \mu_2^*, \dots, \mu_m^*)$, $\rho_i \leq \min(\mu, l_{2i}^*)$ and $l_{2i} \leq l_{1i}^*$, for every $i = 1, 2, \dots, m$, where

$$\rho_i = \max |d_i(t) - p_i|, \quad \forall t \in [t_0, t_1] \quad (48)$$

$$l_{1_i}^* = \frac{3k_1}{8m\rho_i k_4}, \quad l_{2_i}^* = \frac{1}{4m\gamma_{1_i}} \quad \text{and} \quad \mu_i^* = \frac{k_3}{8 \left[\rho_i \gamma_{2_i} + k_4 \left(\frac{L}{m} + \rho_i l_{1_i} \right) \right]^2} \quad (49)$$

such that the system states (Eq. 43) are uniformly bounded. Hence, there exist positive constants B_c and B_d satisfying

$$\|\eta(t)\| \leq B_c, \quad \|\xi(t)\| \leq \|e(t)\| + B_d \quad (50)$$

and a scalar function $\theta(\cdot): \mathbb{R}^m \rightarrow \mathbb{R}$ with the property $\theta(0) = 0$, $\theta(\rho) > 0$, and $\rho_i \neq 0$, for every $i = 1, 2, \dots, m$. Under the initial condition $\|e(0)\| \leq 2\sqrt{mD_2}$, the solution of the system satisfies

$$\|e(t)\| \leq \theta(\rho), \quad \forall t \in [t_0, t_1] \quad (51)$$

where

$$D_2 = \sum_{i=1}^m \rho_i^2 \left[(\gamma_{1_i} B_d + \gamma_{3_i})^2 + (\gamma_{2_i} B_c)^2 \right] \\ \theta(\rho) = \sqrt{\frac{4m\lambda_{\max}(P_s) \sum_{i=1}^m \rho_i^2 \left[(\gamma_{1_i} B_d + \gamma_{3_i})^2 + (\gamma_{2_i} B_c)^2 \right]}{\lambda_{\min}(P_s)}} \quad (52)$$

If a single disturbance enters into the system, then the result of Theorem 1 can be significantly simplified. Consider the nonlinear system (Eq. 1) with a single-input disturbance, that is, in Eq. 43 i is any value of the set $\{1, 2, \dots, m\}$, in which case the regular perturbation system as expressed in Eq. 43 can be written as

$$\begin{aligned} \dot{e} &= A_c e + [d_i(t) - p_i] \Delta A_i(x, p, u) \\ \dot{\eta} &= q(\xi, \eta) + [d_i(t) - p_i] \Delta \phi_i(x, p, u) \\ e_1 &= C e \end{aligned} \quad (53)$$

for every $t \in [t_0, t_1]$, where $d_i \in \Sigma$, $\Delta A_i(\cdot) \in \mathbb{R}^r$, $\Delta \phi_i(\cdot) \in \mathbb{R}^{n-r}$, and i is any value of the set $\{1, 2, \dots, m\}$ ($i = 1$ or $i = 2, \dots$, or $i = m$). Furthermore, the derived results are shown as follows.

Corollary 1. Suppose that the regular perturbation system (Eq. 53) satisfies assumptions 1–4. Then the system states are uniformly bounded and the result of Theorem 1 in Eq. 51 can be reduced as

$$|e_1(t)| \leq \kappa_i \rho_i, \quad \text{as } t \rightarrow \infty \quad (54)$$

where $\kappa_i \geq 0$ and i is any value of the set $\{1, 2, \dots, m\}$,

$$\kappa_i = \sqrt{\frac{4\lambda_{\max}(P_s) \left[(r_{1_i} B_d + r_{3_i})^2 + (r_{2_i} B_c)^2 \right]}{\lambda_{\min}(P_s)}} \quad (55)$$

It is worth noting that the nonlinearity in assumption 4, arising from every input disturbance during every time period, is expressed in terms of the cone-bounded structure. A more useful result can be established if the nonlinearity has a special structure, that is, the nonlinearity arising from the total summation of input disturbances during every time period can be expressed in terms of the cone-bounded structure. This case will be defined as follows.

Assumption 5. The system described in Eq. 43 satisfies the BIBS condition. There exist some suitable positive constants, γ_1^* , γ_2^* , γ_3^* , l_1^* , l_2^* , and l_3^* , for every $t \in [t_0, t_1]$, such that

$$\sum_{i=1}^m \|2P_s \Delta A_i(x, p, u) \circ T^{-1}(\xi, \eta)\| \leq \gamma_1^* \|\xi\| + \gamma_2^* \|\eta\| + \gamma_3^* \quad (56)$$

$$\sum_{i=1}^m \|\Delta \phi_i(x, p, u) \circ T^{-1}(\xi, \eta)\| \leq l_1^* \|\xi\| + l_2^* \|\eta\| + l_3^* \quad (57)$$

for every $x \in \mathbb{R}^n$, $p \in \Pi$ and P_s satisfies the Lyapunov equation (Eq. 32).

Corollary 2. Assume that the plant in Eq. 1 satisfies assumptions 1–3 and 5. Then the system states (Eq. 43) are uniformly bounded. The solution of the system satisfies

$$|e_1(t)| \leq \kappa_0 \rho^*, \quad \text{as } t \rightarrow \infty, \quad (58)$$

where $\rho^* = \max_{i=1}^m |d_i(t) - p_i|$, $\forall t \in [t_0, t_1]$ and

$$\kappa_0 = \sqrt{\frac{4\lambda_{\max}(P_s) \left[(r_1^* B_d + r_3^*)^2 + (r_2^* B_c)^2 \right]}{\lambda_{\min}(P_s)}} \quad (59)$$

In this subsection, several categories of nonlinearity are discussed and the related results of robust stability are obtained. It is important to note that although Theorem 1 provides much useful information, it is not convenient to use the resulting stability analysis in Eq. 51 because it is implicit. However, the results of robust stability in Corollary 1 and Corollary 2 will be useful. Since the inequalities in Eqs. 54 and 58 are explicit functions in their arguments, ρ_i or ρ^* . Although these are relatively simple relationships, stability analysis results will be convenient to use for computing controller parameters. The application of these corollaries for computing controller parameters is established in the following subsection.

Estimation of controller parameter

In light of the results of Corollaries 1 and 2, the problem of developing a suitable method for estimating a controller parameter p_i in the hybrid control law for the purpose of minimizing ρ_i or ρ^* , which is equivalent to minimizing the signal e_1 , naturally arises. We will introduce a simple three-step rule for computing an appropriate tuning parameter for the case of a single-input disturbance. Of course, a similar method can be performed for the case of multiinput disturbances.

Parameter Computing Procedures

Step 1. On the basis of *a priori* estimation and open-loop system simulation for the following unforced system based on Eqs. 1 and 20

$$\dot{x} = \hat{f}(x) = f(x) + g(x)\gamma_0(x,0,0), x(0) = x^s, \quad (60)$$

the constants $P_s, \gamma_1, \gamma_2, \gamma_3, \gamma_1^*, \gamma_2^*, \gamma_3^*, B_d$, and B_c should be first computed.

Step 2. The constant κ_i can be computed from Eq. 55.

Step 3. The iterative procedures for computing p_i are outlined as follows:

- Suppose that the positive or negative sign of d_i is known *a priori*. We suggest that the initial value of a tuning parameter can be chosen as zero. We define

$$p_i(1) = \text{sgn} \left[d_i(t) \right] \frac{|e_1(t)|}{\tau \kappa_i} \Big|_{t=t_c} \quad (61)$$

where the symbol $\text{sgn}(\cdot)$ is a sign function,

$$\begin{aligned} \text{sgn} [d_i(t)] &= +1, \quad \text{if } d_i(t) \geq 0 \\ \text{sgn} [d_i(t)] &= -1, \quad \text{if } d_i(t) < 0 \end{aligned}$$

and $p_i(1)$ represents the first iteration of the tuning parameter based on $t = t_c$ and $t_c \in [t_0, t_1]$. Here τ is a positive parameter, $0 < \tau \leq 1$, and is used for accelerating the convergence of estimation. Notice that the $|e_1|$ signal is obtained from the difference between the plant output and the model output.

- The n th ($n > 1$) iteration of the tuning parameter is constructed in the form of

$$\begin{aligned} p_i(2) &= \text{sgn} \left(d_i(t) \right) \frac{|e_1(t)|}{\tau \kappa_i} \Big|_{t=2t_c} + p_i(1) \\ &\vdots \\ p_i(n) &= \text{sgn} \left(d_i(t) \right) \frac{|e_1(t)|}{\tau \kappa_i} \Big|_{t=nt_c} + p_i(n-1) \end{aligned} \quad (62)$$

- If the error $|p_i(n-1) - p_i(n)| \leq$ an error tolerance, then the iterative procedure is complete.

A detailed computing flow chart for parameter computing procedures is given in Figure 2. Consequently, we will show that such a parameter computed from the just-mentioned procedures will achieve some degree of nonlinearity cancellation. This property is summarized as follows. Before we proceed to state this property, the input-output model of Eq. 43 is required *a priori*.

Proposition 1. Assume that the system (Eq. 43) satisfies assumption 2, and d_i and ΔA_{i_j} , for every $i = 1, 2, \dots, m$ and $j = 1, 2, \dots, r$ are continuously differentiable. Then the input-output model can be expressed in the following form

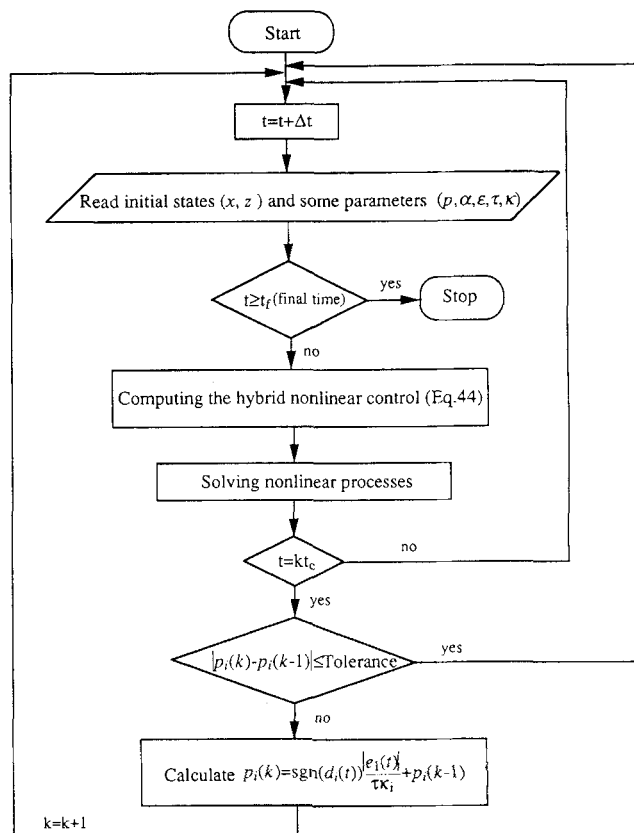


Figure 2. Flow chart of computing controller parameters.

$$\begin{aligned} e_1^{(r)} + \alpha_r e_1^{(r-1)} + \dots + \alpha_1 e_1 &= \sum_{i=1}^m \left[\sum_{j=1}^r \left(\vartheta_i(t) \Delta A_{i_j}^{(r-j)}(x, p, u) \right. \right. \\ &+ \vartheta_i(t)^{(r-i)} \Delta A_{i_j}(x, p, u) \Big) + \sum_{j=1}^r \alpha_j \sum_{k=1}^j \left(\vartheta_i(t) \Delta A_{i_k}^{(j-k)}(x, p, u) \right. \\ &\left. \left. + \vartheta_i(t)^{(j-k)} \Delta A_{i_k}(x, p, u) \right) \right] \end{aligned} \quad (63)$$

where $\vartheta_i(t) = d_i(t) - p_i$, for every $i = 1, 2, \dots, m$ and $t \in [t_0, t_1]$.

Proposition 2. After a sufficient number of times computing procedures based on the previous parameter computing method, the absolute error signal $|e_1|$ can converge to a sufficiently small size. Then, the parameter p_i , where i is any value of the set $\{1, 2, \dots, m\}$, exists and is bounded.

A similar computing method can be performed for the case of multiinput disturbances. First our treatment method is to compute a single parameter instead of a series of parameters of the controller. Second we follow similar procedures as described in step 1 and step 2, but replace the calculation of k_i with that of k_0 as shown in Eq. 58. Since we only have the information, e_1 , we can only compute a controller parameter during a computing cycle like step 1–step 3. Intuitively, the best choice of i of p_i is the dominant direction of the multi-input disturbances. Such a choice should achieve the maxi-

Table 1. Dimensionless Group for the CSTR Model

$\psi = \frac{E}{RT_{rf0}}$	$D_a = k_0 \tau_0 \exp(-\psi)$	$\beta_r = \frac{UA}{\rho_{O_j} C_{p_r} F_r}$
$\beta_c = \frac{UA(T_r - T_j) V_j}{\rho_{O_j} C_{p_j} F_r V_r}$	$B = \frac{(-\Delta H) C_{A_{f0}}}{\rho_{O_j} C_{p_r} T_{rf0}}$	$x_{3f} = \frac{T_{jf0} - T_{rf0}}{T_{rf0}} \psi$
Dimensionless time	$t = \frac{t^*}{\tau_0}$	
Dimensionless concentration	$x_1 = 1 - \frac{C_A}{C_{A_{f0}}}$	
Dimensionless reactor temperature	$x_2 = \frac{T_r - T_{rf0}}{T_{rf0}} \psi$	
Dimensionless cooling jacket temperature	$x_3 = \frac{T_j - T_{rf0}}{T_{rf0}} \psi$	
Dimensionless manipulated input	$u = \frac{V_r/F_r}{V_j/F_j}$	
Inlet stream concentration	$d_1 = 1 - \frac{C_{A_f}}{C_{A_{f0}}}$	
Inlet stream temperature	$d_2 = \frac{T_{rf} - T_{rf0}}{T_{rf0}} \psi$	
Inlet cooling stream temperature	$d_3 = \frac{T_{jf} - T_{jf0}}{T_{rf0}} \psi$	

imum degree of nonlinearity cancellation. An illustrative example will demonstrate these features in the next section.

Application

A first-order exothermic reaction $A \rightarrow B$ carried out in a CSTR is mathematically modeled by

$$\begin{aligned} \frac{dC_A}{dt^*} &= \frac{F_r}{V_r} (C_{A_f} - C_A) - k_0 \exp(-E/RT_r) C_A \\ \frac{dT_r}{dt^*} &= \frac{F_r}{V_r} (T_f - T_r) - \frac{(\Delta H)}{\rho_{O_r} C_{p_r}} k_0 \exp(-E/RT_r) C_A \\ &\quad - \frac{UA(T_r - T_j)}{\rho_{O_r} C_{p_r} V_r} \\ \frac{dT_j}{dt^*} &= \frac{F_j}{V_j} (T_{jf} - T_j) + \frac{UA(T_r - T_j)}{\rho_{O_j} C_{p_j} V_j} \end{aligned} \quad (64)$$

where C_A is reactant concentration, T is temperature, V is volume, F is flow rate, ρ_o is density, and C_p is heat capacity. Reactor and cooling jacket values are denoted by subscripts r and j , respectively, and the inlet feed values are denoted by subscript f . The remaining notation is defined in the Notation section and the detailed formulations are also shown in Poslavsky and Kantor (1991).

The system (Eq. 64) can be written in the following dimensionless form:

$$\dot{x}_1 = -x_1 + D_a(1 - x_1) \exp \left[x_2 / \left(1 + \frac{x_2}{\psi} \right) \right] + d_1$$

$$\begin{aligned} \dot{x}_2 &= -x_2 + BD_a(1 - x_1) \exp \left[x_2 / \left(1 + \frac{x_2}{\psi} \right) \right] \\ &\quad - \beta_r(x_2 - x_3) + d_2 \\ \dot{x}_3 &= \beta_c(x_2 - x_3) + (x_{3f} - x_3)u + d_3 u \end{aligned} \quad (65)$$

where the dimensionless variables and parameters are defined in Table 1. The control goal is to regulate reactor temperature x_2 at its setpoint value, that is, $\lim_{t \rightarrow \infty} x_2(t) = y_{sp}$, by manipulating the cooling stream flow rate u . The nominal system parameters and operating condition used in numerical simulations are

$$B = 8, \quad D_a = 0.14, \quad \psi = 20, \quad \beta_c = 1.5, \quad \beta_r = 1.5, \quad x_{3f} = -4.$$

If we set $u^d = 0.97$, we can obtain a stationary operating point as initial conditions, $x_1^d = 0.65$, $x_2^d = 3$, and $x_3^d = 0.25$.

The unmeasurable disturbances (Eq. 65) can be formulated as

$$\sum_{i=1}^3 \omega_i(x, u) d_i(t) = \begin{bmatrix} 1 \\ 0 \\ 0 \end{bmatrix} d_1 + \begin{bmatrix} 0 \\ 1 \\ 0 \end{bmatrix} d_2 + \begin{bmatrix} 0 \\ 0 \\ u \end{bmatrix} d_3. \quad (66)$$

Here, d_1 , d_2 , and d_3 are considered as the constant step change, so the resulting perturbed equilibrium point still exists in the neighborhood of the nominal operating point. Using the previous design algorithms in Eqs. 8–10 and assumption 1, we first consider the design model with tuning parameters as follows:

$$\dot{x} = f_d[x, p^*(t), u] + g(x)u \quad (67)$$

where

$$f_d(x, p, u) = \begin{bmatrix} -x_1 + D_a(1-x_1) \exp \left[x_2 / \left(1 + \frac{x_2}{\psi} \right) \right] + p_1^*(t) \\ -x_2 + BD_a(1-x_1) \exp \left[x_2 / \left(1 + \frac{x_2}{\psi} \right) \right] - \beta_r(x_2 - x_3) + p_2^*(t) \\ \beta_c(x_2 - x_3) + p_3^*(t)u \end{bmatrix} \quad (68)$$

$$g(x) = \begin{bmatrix} 0 \\ 0 \\ x_{3_f} - x_3 \end{bmatrix}.$$

Let us choose the coordinate transformations with parameters during every time period, that is, $t \in [t_0, t_1]$:

$$T(x, p) = [\xi_1 \quad \xi_2 \quad \eta]^T = [x_2 \quad L_{f_d}x_2 \quad x_1]^T, \quad (69)$$

which transforms Eq. 72 into the following form

$$\begin{aligned} \dot{\xi}_1 &= \xi_2 \\ \dot{\xi}_2 &= L_{f_d}^2 x_2 + u L_g L_{f_d} x_2 \\ \dot{\eta} &= q(\xi, \eta) \\ y &= x_2 = \xi_1, \end{aligned} \quad (70)$$

where $q(\xi, \eta) = -\eta + D_a(1-\eta) \exp[\xi_1/(1+(\xi_1/\psi))] + p_1$. Moreover, the zero dynamics can be described in the form of

$$\dot{\eta} = -(1 + D_a)\eta + D_a + p_1. \quad (71)$$

It is clear that the zero dynamics is exponentially stable for initial condition $\eta(0) \geq [(D_a + p_1)/(1 + D_a)]$. By definition, this design model is minimum-phase and has relative degree two. Second, we select a controllable model as an internal model for output regulation.

$$\begin{aligned} \dot{z}_1 &= z_2 \\ \dot{z}_2 &= c_1 z_1 + c_2 z_2 + \nu_d \\ y_m &= z_1 \end{aligned} \quad (72)$$

where $z_1(0) = \xi_1(0)$, $z_2(0) = \xi_2(0)$, c_1 and c_2 are the known constants, and ν_d is the input signal. As defined in Eq. 34, the parameterized feedback is

$$\nu_d = \epsilon^{-2} [\alpha_1(y_{sp} - y + y_m) - \epsilon^2(c_1 z_1 + c_2 z_2) - \alpha_1 z_1 - \alpha_2 \epsilon z_2]. \quad (73)$$

Furthermore, a *hybrid* nonlinear controller is constructed as

$$\begin{aligned} (L_{f_d}^2 x_2) + u(L_g L_{f_d} x_2) &= \nu \\ \nu &= \epsilon^{-2} \alpha_1(y_{sp} - y + y_m) + \alpha_1[(1 - \epsilon^{-2})z_1 - \xi_1] \\ &\quad + 2\sqrt{\alpha_1}[(1 - \epsilon^{-1})z_2 - \xi_2], \end{aligned} \quad (74)$$

where

$$\begin{aligned} L_g L_{f_d} x_2 &= \beta_r(x_{3_f} - x_3) + p_3 \\ L_{f_d}^2 x_2 &= [-BD_a w(x_2)][-x_1 + D_a(1-x_1)w(x_2) + p_1] \\ &\quad + [-1 + BD_a(1-x_1)w(x_2)(1 + x_2/\psi)^{-2} - \beta_r] \\ &\quad \times [-x_2 + BD_a(1-x_1)w(x_2) - \beta_r(x_2 - x_3) + p_2] \\ &\quad + \beta_r[\beta_c(x_2 - x_3)] \end{aligned} \quad (75)$$

and $w(x_2) = \exp[x_2/(1+(x_2/\psi))]$. We must carefully select the parameter p_3 to make sure that the term, $[\beta_r(x_{3_f} - x_3) + p_3]$, is not zero as long as $p_3 \neq -\beta_r[x_{3_f} - x_3(t)]$ for every $t \in [t_0, t_1]$. Thus, we obtain the specified closed-loop system for every $t \in [t_0, t_1]$ as follows:

$$\begin{aligned} \begin{bmatrix} \dot{e}_1 \\ \dot{e}_2 \end{bmatrix} &= \begin{bmatrix} 0 & 1 \\ -\alpha_1 & -\alpha_2 \end{bmatrix} \begin{bmatrix} e_1 \\ e_2 \end{bmatrix} + \sum_{i=1}^3 (d_i - p_i) \Delta A_i \\ \dot{\eta} &= q(\xi, \eta) + \sum_{i=1}^3 (d_i - p_i) \Delta \phi_i \\ e_1 &= Ce, \end{aligned} \quad (76)$$

where $e_1 = x_2 - z_1$, $e_2 = \xi_2 - z_2$, $C = [1, 0]$,

$$\begin{aligned} \Delta A_1 &= \begin{bmatrix} 0 \\ -BD_a w(x_2) \end{bmatrix}, \\ \Delta A_2 &= \begin{bmatrix} 1 \\ -1 + BD_a(1-x_1)w(x_2) \left(1 / \left(1 + \frac{x_2}{\psi} \right)^2 \right) - \beta_r \end{bmatrix}, \\ \Delta A_3 &= \begin{bmatrix} 0 \\ \beta_r u \end{bmatrix}, \quad \Delta \phi_1 = 1, \quad \text{and} \quad \Delta \phi_2 = \Delta \phi_3 = 0. \end{aligned} \quad (77)$$

Here, we consider the coefficients $(c_1, c_2) = (4, 4)$ for the internal model (Eq. 72), and $\alpha_1 = 1$ for the control (Eq. 74).

Thus, we calculate $P_s = \begin{bmatrix} P_{s_1} & P_{s_2} \\ P_{s_3} & P_{s_4} \end{bmatrix}$, which satisfies the following Lyapunov equation:

$$\begin{aligned} \begin{bmatrix} 0 & 1 \\ -\alpha_1 & -2\sqrt{\alpha_1} \end{bmatrix}^T \begin{bmatrix} P_{s_1} & P_{s_2} \\ P_{s_3} & P_{s_4} \end{bmatrix} \\ + \begin{bmatrix} P_{s_1} & P_{s_2} \\ P_{s_3} & P_{s_4} \end{bmatrix} \begin{bmatrix} 0 & 1 \\ -\alpha_1 & -2\sqrt{\alpha_1} \end{bmatrix} &= \begin{bmatrix} -1 & 0 \\ 0 & -1 \end{bmatrix}. \end{aligned}$$

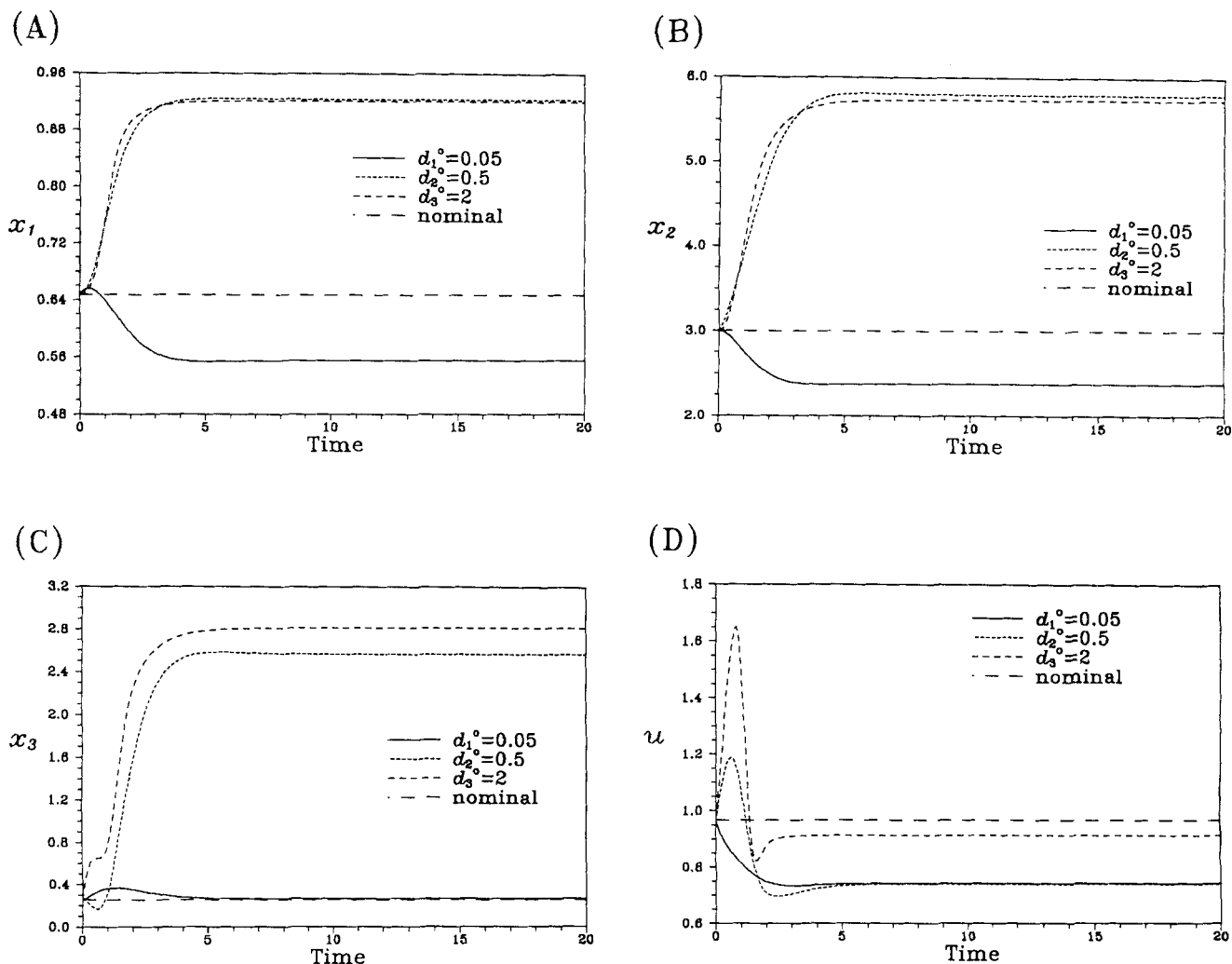


Figure 3. (a) Response of state x_1 under the maximum disturbance $d_1^0 = 0.05$, $d_2^0 = 0.5$, and $d_3^0 = 2$, respectively; (b) response of state x_2 under the maximum disturbance $d_1^0 = 0.05$, $d_2^0 = 0.5$, and $d_3^0 = 2$, respectively; (c) response of state x_3 under the maximum disturbance $d_1^0 = 0.05$, $d_2^0 = 0.5$, and $d_3^0 = 2$, respectively; (d) response of manipulated input u under the maximum disturbance $d_1^0 = 0.05$, $d_2^0 = 0.5$, and $d_3^0 = 2$.

Thus, we obtain $P_s = \begin{bmatrix} 1.25 & 0.5 \\ 0.5 & 0.25 \end{bmatrix}$. Therefore, the maximum (minimum) eigenvalue of P_s can be shown as

$$\lambda_{\max}(P_s) = \frac{3+2\sqrt{2}}{4} \quad \text{and} \quad \lambda_{\min}(P_s) = \frac{3-2\sqrt{2}}{4}.$$

Next, we will provide a series of numerical simulation results for this reactor system based on the nonlinear controller (Eq. 74). Here we consider the external disturbances, including concentration, reactor temperature, and temperature perturbation of the cooling jacket, that exist alone or simultaneously in the CSTR process. Observing the advance simulation results, we find that the manipulated input response is smooth when $\alpha_1 = \epsilon = 1$ is used. Practically, the bounded control action, $|u| \leq 3$, is set.

Single-input disturbance rejection

We consider the case of a single disturbance entered into the system. Suppose that the bounded disturbance is described as $|d_1| \leq 0.05$, or $|d_2| \leq 0.5$, or $|d_3| \leq 2$. First, we select the maximum values, $d_1^0 = 0.05$, $d_2^0 = 0.5$, and $d_3^0 = 2$, respectively, to perform off-line simulation for the unforced CSTR system based on the nominal operating point. Figure 3 shows that the system is stable and is bounded in maximum d^0 . Second, we shall estimate the constants γ_1 , γ_2 , γ_3 , B_d , and B_c based on Figure 3. Thus, we consider that a single disturbance d_1 existed in the system, by assumption 4, so the bounds can be described as

$$\|2P_s \Delta A_1 \circ T^{-1}(\xi, \eta)\| = 1.12 \left\| B D_a \exp \left(\frac{\xi_1}{1 + \xi_1/\psi} \right) \right\| \leq \gamma_1 \|\xi\| + \gamma_2 \|\eta\| + \gamma_3.$$

Using the Taylor expansion in $\xi_1(0) = 0$ and $\eta(0) = 0$, we obtain

$$\gamma_{1_1} = 1.12 \times BD_a \exp \left(\frac{\xi_1}{1 + \xi_1/\psi} \right) \left[\frac{1}{\left(1 + \frac{\xi_1}{\psi} \right)^2} \right] \bigg|_{\xi_1=0} = 1.66,$$

$$\gamma_{2_1} = 0$$

and

$$\gamma_{3_1} = 1.12 \times BD_a \exp \left(\frac{\xi_1}{1 + \xi_1/\psi} \right) \bigg|_{\xi_1=0} = 1.66.$$

From Figures 3b and 3c, estimating $|\xi_1 - \xi_1^d| = 0.62$ and $|\xi_2 - \xi_2^d| = 0$ yields

$$\|\xi\| \leq \left\| \begin{matrix} 0.62 \\ 0 \end{matrix} \right\| = 0.62 = B_d,$$

and selecting $|\eta - \eta^d| = 0.09$ from Figure 3a, we obtain $\|\eta\| \leq 0.09 = B_c$. Therefore, from the result of Corollary 1, we select a suitable constant

$$\kappa_1 = \sqrt{\frac{4\lambda_{\max}(P_s) [(\gamma_{1_1}B_d + \gamma_{3_1})^2 + (\gamma_{2_1}B_c)^2]}{\lambda_{\min}(P_s)}} = 31.35.$$

Similarly, if a single disturbance d_2 existed in the system, by assumption 4, the bounds can be described as

$$\|2P_s \Delta A_2 \circ T^{-1}(\xi, \eta)\| = 1.12 \left| -1 + BD_a(1 - x_1) \exp \left(\frac{\xi_1}{1 + \xi_1/\psi} \right) \left(\frac{1}{\left(1 + \frac{\xi_1}{\psi} \right)^2} \right) - \beta_r \right| + 2.69.$$

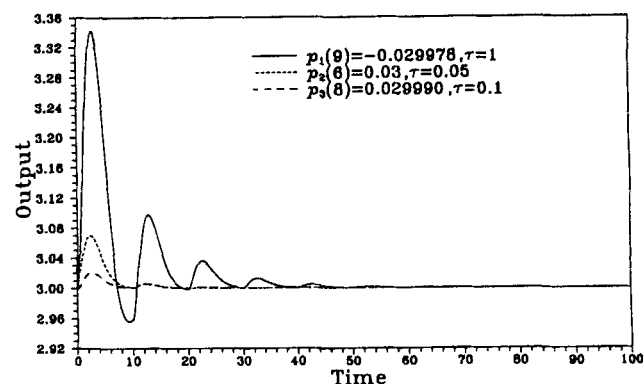
Using the Taylor expansion in $\xi_1(0) = 0$ and $\eta(0) = 0$, we obtain $\gamma_{1_1} = 1.49$, $\gamma_{2_2} = 1.66$, and $\gamma_{3_2} = 3.83$. From Figure 3a, 3b, and 3c, and estimating $|\xi_1 - \xi_1^d| = 2.8$, $|\xi_2 - \xi_2^d| = 0.5$, and $|\eta - \eta^d| = 0.27$, we get $\|\xi\| \leq 2.84 = B_d$ and $\|\eta\| \leq 0.27 = B_c$. Therefore, from the result of Corollary 1, we select a suitable constant $\kappa_2 = 94.12$. For the other disturbance d_3 , based on Figure 3d, we can estimate

$$\|2P_s \Delta A_3 \circ T^{-1}(\xi, \eta)\| = 1.12 |\beta_r u| \leq \gamma_{3_3}$$

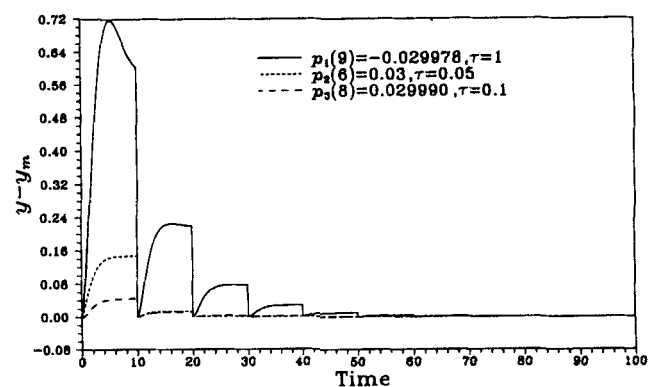
and select $\gamma_{1_3} = 0$, $\gamma_{2_3} = 0$, and $\gamma_{3_3} = 1.68$. Therefore, from the result of Corollary 1, we obtain $\kappa_3 = 19.58$. Finally, we follow the parameter computing procedures described in Eq. 61 to compute p_1 , p_2 , and p_3 . We will provide a series of numerical simulations for a single disturbance d_1 , or d_2 or d_3 , entered into the system to evaluate the versatility of the proposed method.

(1) Figure 4 shows that the system uses the ability of the closed-loop system to reject disturbances based on the hybrid control law in Eq. 74 and the piecewise dynamic behaviors of

(A)



(B)



(C)

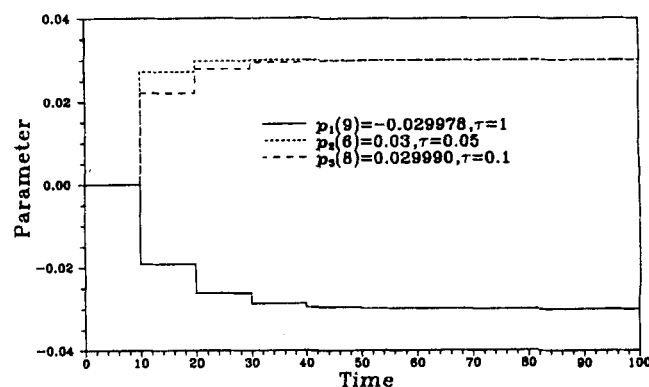


Figure 4. (a) Concentration response under a single-input disturbance $d_1 = -0.03$, $d_2 = 0.03$, and $d_3 = 0.03$, respectively; (b) corresponding response of the plant/model mismatch ($y - y_m$); (c) dynamical profile of tuning parameter p_1 , p_2 , and p_3 , respectively.

tuning parameters. As shown in Figure 4a, the output responses have no steady-state errors and asymptotically achieve disturbance rejection. The corresponding mismatches between the plant output and the internal model output are plotted in Figure 4b. Figure 4c shows the corresponding dynamical profiles of tuning parameters p_1 , p_2 , and p_3 .

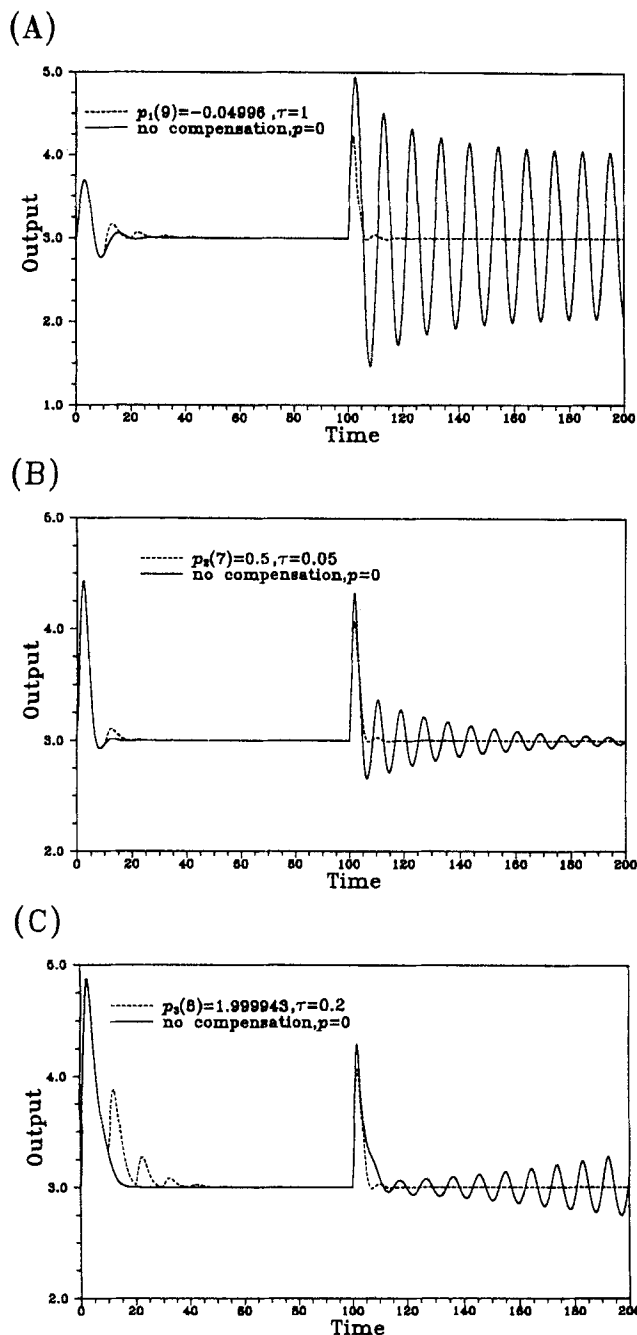


Figure 5. (a) Concentration response under a single-input disturbance $d_1 = -0.05$ at $t = 0$, and parameter perturbations of 3% in B and D_a after $t = 100$; (b) concentration response under a single-input disturbance $d_2 = 0.5$ at $t = 0$, and parameter perturbations of 3% in B and D_a after $t = 100$; (c) concentration response under a single-input disturbance $d_3 = 2$ at $t = 0$, and parameter perturbations of 3% in B and D_a after $t = 100$.

(2) Figure 5 shows that the system uses the robustness of the controller with respect to the modeling errors. It is evident from Figures 5a, 5b, and 5c that the output responses with dashed lines have no steady-state errors and asymptoti-

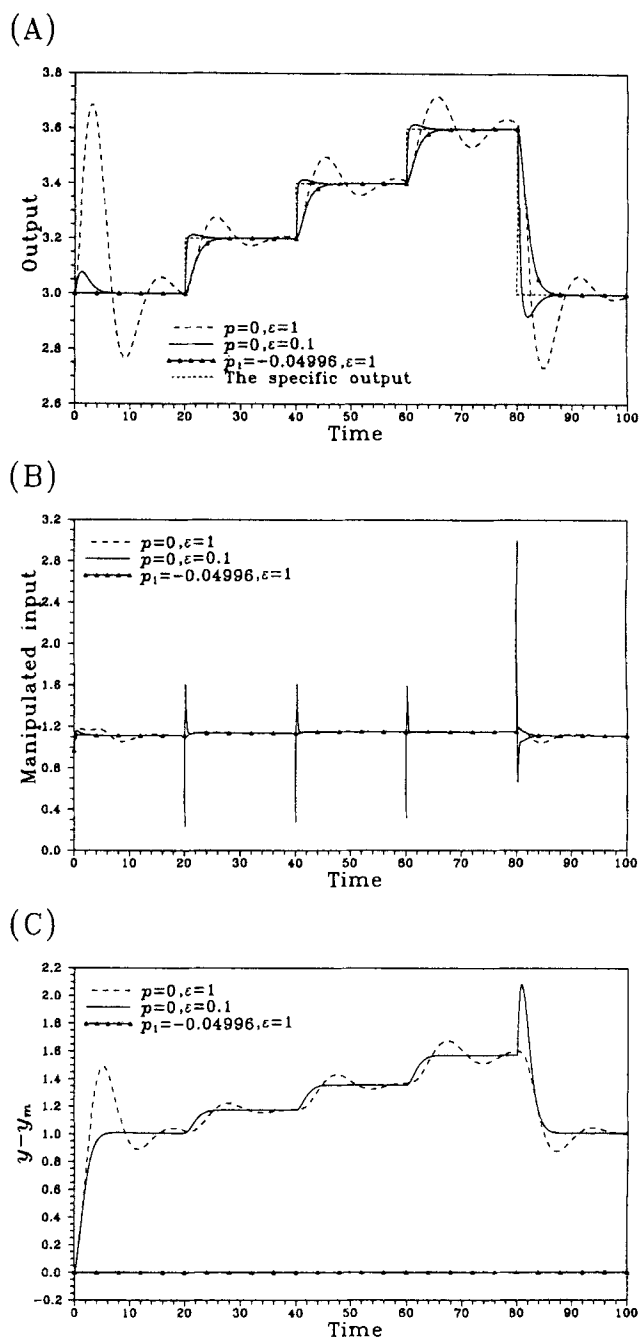


Figure 6. (a) Concentration response under a positive and negative setpoint step change with a single-input disturbance $d_1 = -0.05$; (b) corresponding manipulated input u ; (c) corresponding response of the plant/model mismatch ($y - y_m$).

cally achieve disturbance rejection for a single-input disturbance $d_1 = -0.05$, $d_2 = 0.5$, and $d_3 = 2$, respectively, initially entering into the plant, and after $t = 100$ the plant having 3% parametric perturbations in B and D_a . Notice that the output responses with solid lines, which suggest the controller parameters, show the oscillating characteristics in Figures 5a and 5b, and the divergent phenomenon in Figure 5c.

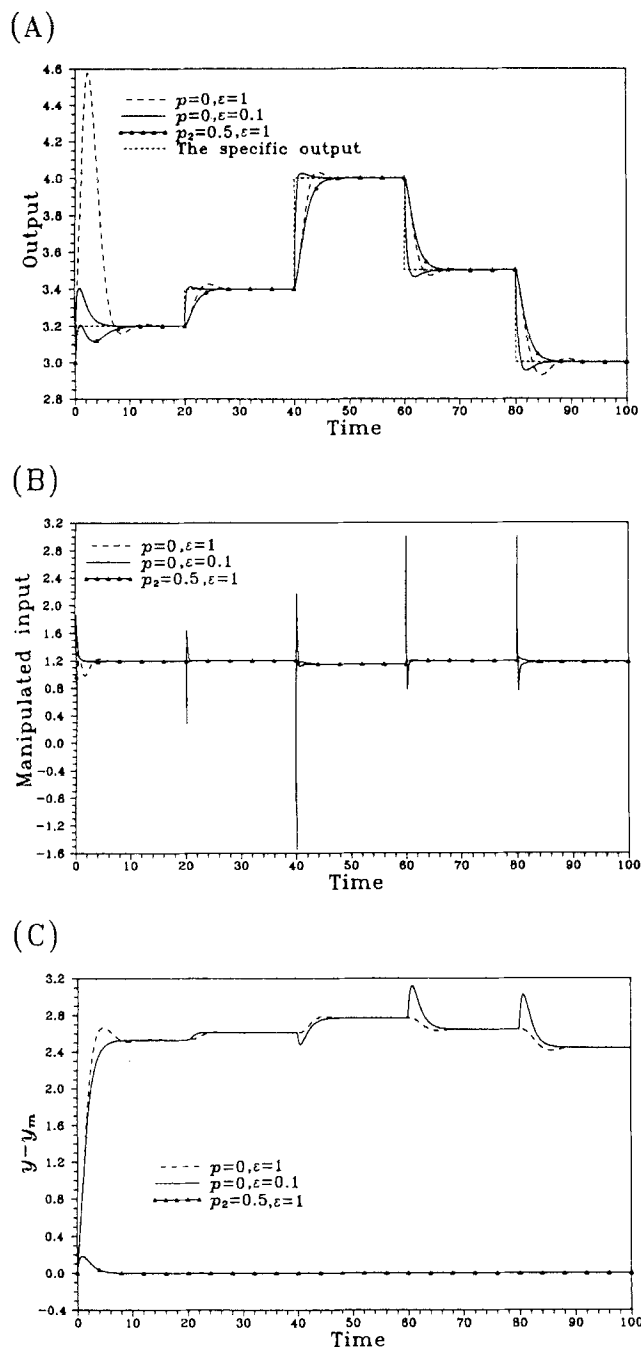


Figure 7. (a) Concentration response under a positive and negative setpoint step change with a single-input disturbance $d_2 = 0.5$; (b) corresponding manipulated input u ; (c) corresponding response of the plant/model mismatch ($y - y_m$).

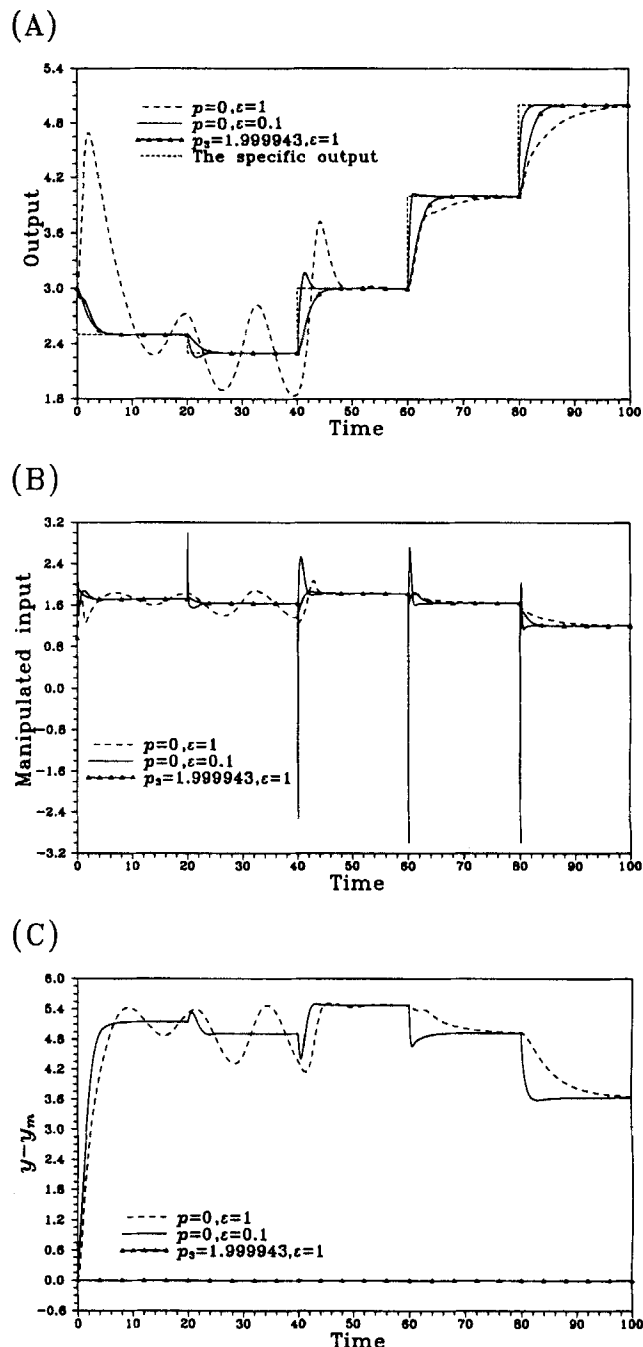


Figure 8. (a) Concentration response under positive and negative setpoint step change with a single-input disturbance $d_2 = 2$; (b) corresponding manipulated input u ; (c) corresponding response of plant/model mismatch ($y - y_m$).

The excellent robustness property of the hybrid control law is verified by these simulation results.

(3) Figures 6, 7, and 8 show the system responses for the ability of the closed-loop system to track a positive and negative setpoint change on the basis of the previous computing results, $p_1 = -0.04996$, $p_2 = 0.5$, and $p_3 = 1.999943$, for a single-input disturbance, $d_1 = -0.05$, $d_2 = 0.5$, and $d_3 = 2$,

respectively. A series of setpoint changes are illustrated in Table 2. It can be seen from Figures 6a, 7a, and 8a that the output responses of our proposed method (solid line with triangular marks) have satisfactory output regulation. The solid lines represent the high-gain control, that is, the case of $\epsilon = 0.1$, without performing the parameter estimation. For this reason, these cases (solid line with triangular marks) have

Table 2. Test Signal Applied for Controller Evaluation in the Case of Single-Input Disturbance

Time	Step change for $d_1 = -0.05$ (Figure 6a)	Step change for $d_2 = 0.5$ (Figure 7a)	Step change for $d_3 = 2$ (Figure 8a)
0	$y_{sp} = 3.0$	$y_{sp} = 3.2$	$y_{sp} = 2.5$
20	$y_{sp} = 3.2$	$y_{sp} = 3.4$	$y_{sp} = 2.3$
40	$y_{sp} = 3.4$	$y_{sp} = 4.0$	$y_{sp} = 3.0$
60	$y_{sp} = 3.6$	$y_{sp} = 3.5$	$y_{sp} = 4.0$
80	$y_{sp} = 3.0$	$y_{sp} = 3.0$	$y_{sp} = 5.0$

fewer mismatches than those cases represented by the dashed line, as shown in Figures 6c, 7c, and 8c, respectively. Although the case of high-gain control ($p = 0$ and $\epsilon = 0.1$) has a large plant/model mismatch, by the analysis of Eqs. 35 and 36 it still has the best output tracking response. The cost of this performance is high control activity, as shown in Figures 6b, 7b and 8b, respectively.

Multiinput disturbances rejection

Here we consider that the external disturbances with boundedness, $\|d\| \leq 0.05$, simultaneously enters into the CSTR reactor system. First, we select the maximum values $d_1^0 = d_2^0 = d_3^0 = 0.05$ to perform off-line simulation for the unforced CSTR system based on a nominal condition. Figure 9 shows that the system is open-loop stable and is bounded in maximum d^0 . Second, we need to estimate constants γ_1^* , γ_2^* , γ_3^* , B_d , and B_c based on Figure 9. Thus, we see that multiple disturbances existed in the system, by assumption 5 and using the Taylor expansion at $\xi_1(0) = 0$ and $\eta(0) = 0$, so the bounds can be described as

$$\sum_{i=1}^3 \|2P_s \Delta A_i \circ T^{-1}(\xi, \eta)\| \leq (1.66 + 1.49)\|\xi\| + 1.66\|\eta\| + (3.83 + 1.66 + 1.68).$$

We can select $\gamma_1^* = 3.15$, $\gamma_2^* = 1.66$, and $\gamma_3^* = 7.17$. From

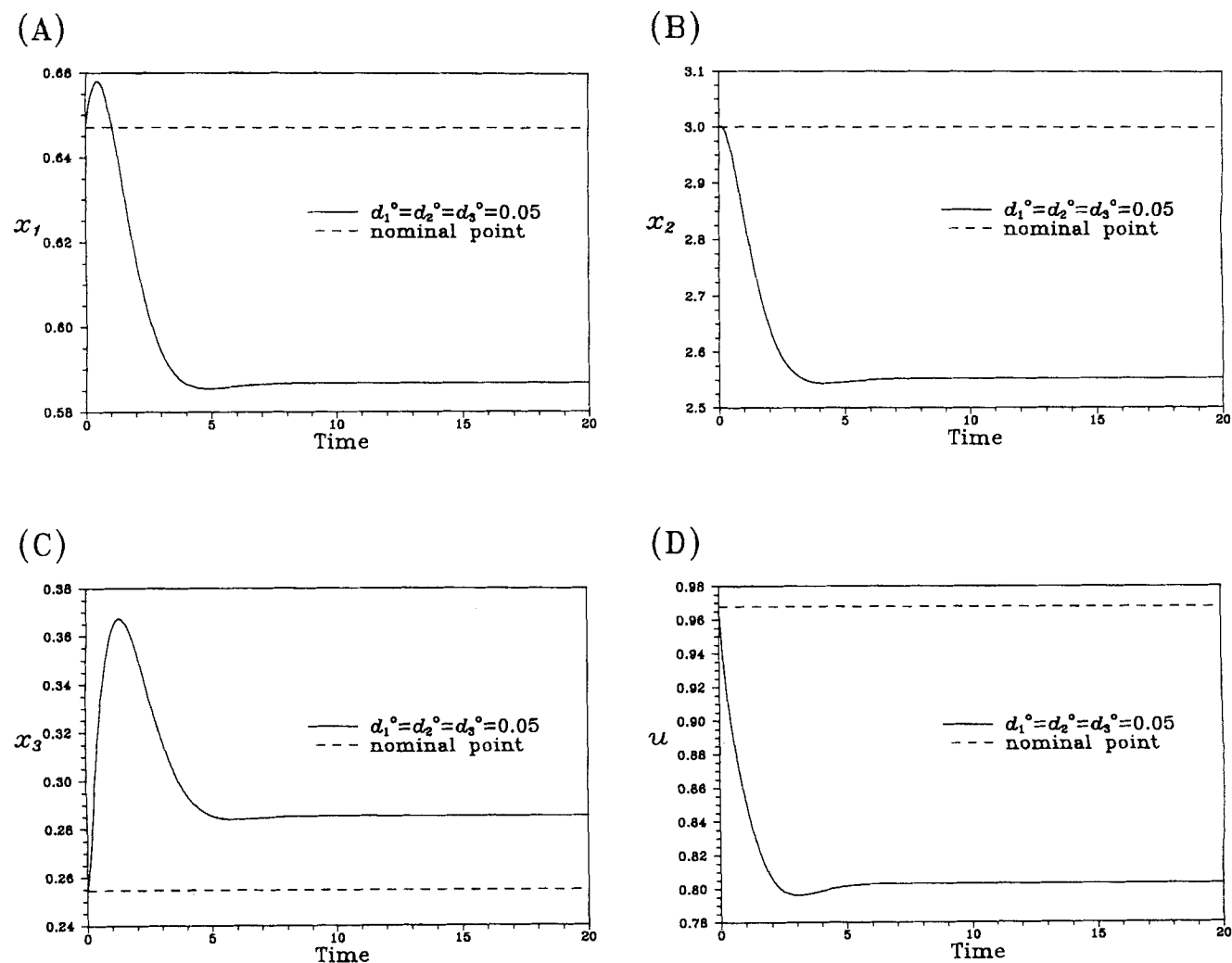


Figure 9. (a) Response of state x_1 under the maximum disturbances $d_1^0 = d_2^0 = d_3^0 = 0.05$; (b) response of state x_2 under the maximum disturbances $d_1^0 = d_2^0 = d_3^0 = 0.05$; (c) response of state x_3 under the maximum disturbances $d_1^0 = d_2^0 = d_3^0 = 0.05$; (d) response of the manipulated input u under the maximum disturbances $d_1^0 = d_2^0 = d_3^0 = 0.05$.

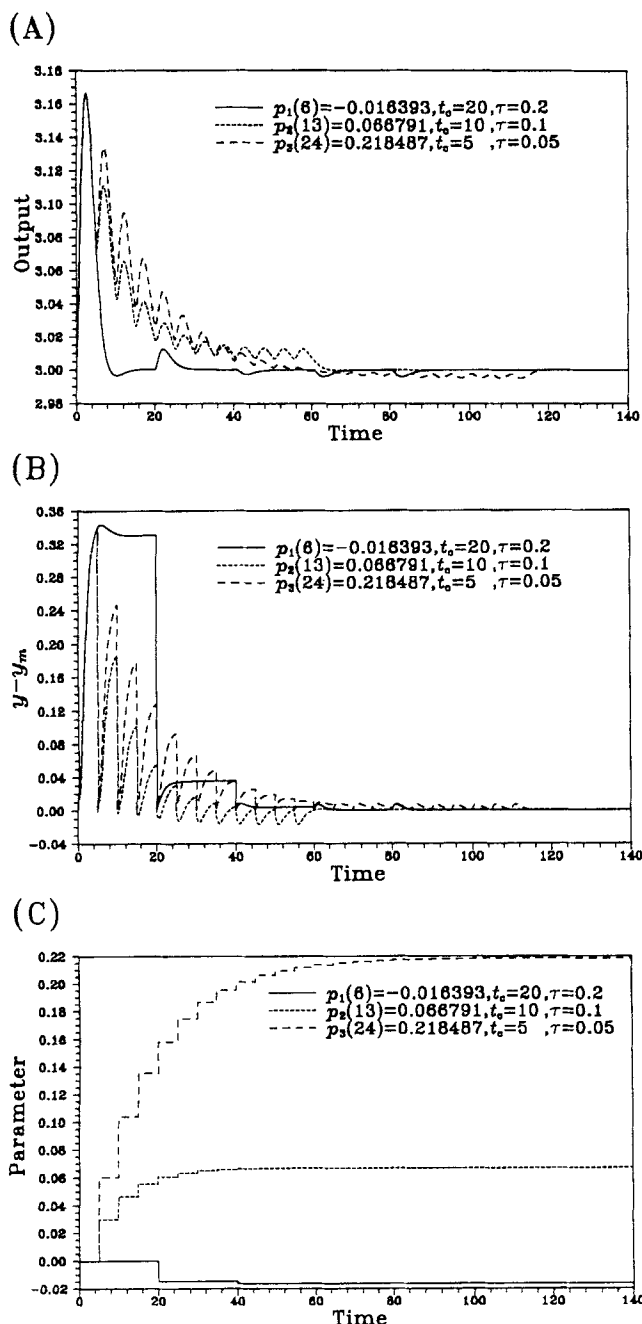


Figure 10. (a) Concentration response under multiinput disturbances $(d_1, d_2, d_3) = (-0.01, 0.02, 0.02)$; (b) corresponding response of plant/model mismatch $(y - y_m)$; (c) dynamical profile of tuning parameter p_1, p_2 , and p_3 .

Figures 9b and 9c and estimating $|\xi_1 - \xi_1^d| = 0.447$ and $|\xi_2 - \xi_2^d| = 0.05$, yields $\|\xi\| \leq 0.45 = B_d$, and from Figure 9a selecting $|\eta - \eta^d| = 0.07$, we obtain $\|\eta\| \leq 0.07 = B_c$. Therefore, from the result of Corollary 2 we select a suitable constant $\kappa_0 = 100.11$. Finally, we follow the parameter computing procedures to compute p_1, p_2 , and p_3 , respectively.

(4) Figure 10 shows that the system uses the ability of the closed-loop system to reject disturbances based on the hybrid

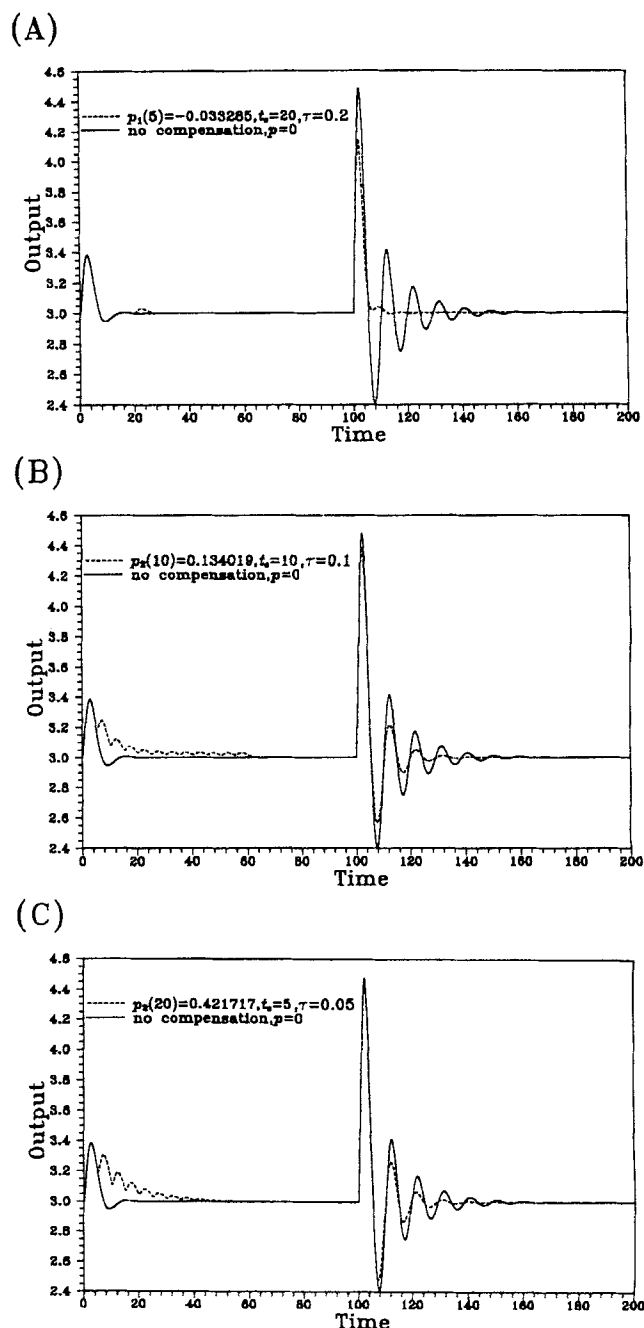


Figure 11. (a) Concentration response under multiinput disturbances $(d_1, d_2, d_3) = (-0.03, 0.01, 0.01)$ at $t = 0$, and parameter perturbations of 3% in B and D_a after $t = 100$; (b) concentration response under multiinput disturbances $(d_1, d_2, d_3) = (-0.03, 0.01, 0.01)$ at $t = 0$, and parameter perturbations of 3% in B and D_a after $t = 100$; (c) concentration response under multiinput disturbances $(d_1, d_2, d_3) = (-0.03, 0.01, 0.01)$ at $t = 0$, and parameter perturbations of 3% in B and D_a after $t = 100$.

control law in Eq. 74 and the piecewise dynamic behaviors of tuning parameters. As shown in Figure 10a, the output responses have no steady-state errors and asymptotically

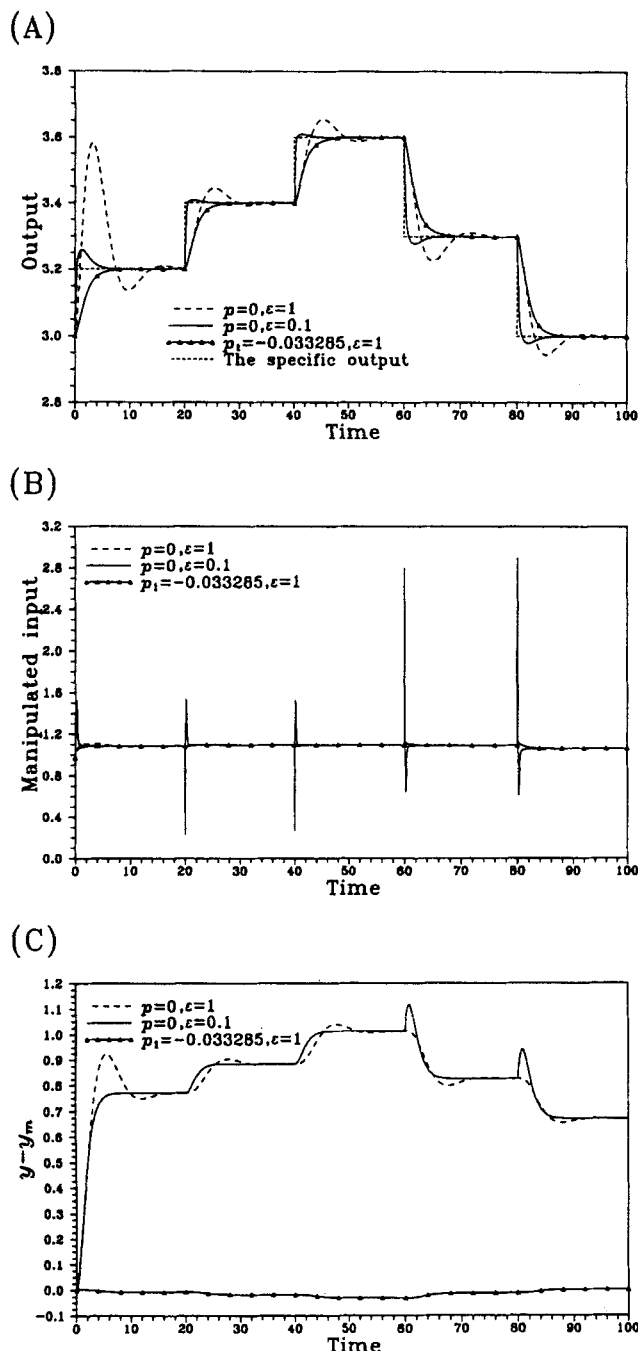


Figure 12. (a) Concentration response under a positive and negative setpoint step change with multiinput disturbances $(d_1, d_2, d_3) = (-0.03, 0.01, 0.01)$; (b) corresponding manipulated input u ; (c) corresponding response of the plant/model mismatch $(y - y_m)$.

achieve disturbance rejection. The corresponding mismatches between the plant output and the internal model output are plotted in Figure 10b. Figure 10c shows the corresponding dynamical profiles of tuning parameters p_1 , p_2 , and p_3 .

(5) Figure 11 shows that the system uses the robustness of the controller with respect to modeling errors. It is evident from Figures 11a, 11b and 11c that the output responses

Table 3. Test Signal Applied for Controller Evaluation in the Case of Multiinput Disturbances

Time	Step Change
0	$y_{sp} = 3.2$
20	$y_{sp} = 3.4$
40	$y_{sp} = 3.6$
60	$y_{sp} = 3.3$
80	$y_{sp} = 3.0$

(dashed lines) have no steady-state errors and asymptotically achieve disturbance rejection for multiinput disturbances $(d_1, d_2, d_3) = (-0.03, 0.01, 0.01)$, initially entering into the plant, and after $t = 100$ the plant having 3% parametric perturbations in B and D_a . Notice that the output responses (solid lines, which do not perform the parameter estimation) show the large oscillating characteristics as shown in Figure 11a, 11b, and 11c. The good robustness property of the hybrid control law is verified by these simulation results.

(6) Figure 12 shows the system responses for the ability of the closed-loop system to track a positive and negative setpoint change by using previous results, $p_1 = -0.033285$ and $(d_1, d_2, d_3) = (-0.03, 0.01, 0.01)$. A series of setpoint changes is shown in Table 3. Figure 12a shows that the output responses of our proposed method (solid line with triangular marks) have satisfactory output regulation. The solid line represents the high-gain control, that is, the case of $\epsilon = 0.1$, without performing the parameter estimation. For this reason, the case (solid line with triangular marks) has a smaller mismatch than that of the case represented by the dashed line, as shown in Figure 12c. Although the case of high-gain control ($p = 0$ and $\epsilon = 0.1$) has a large plant/model mismatch, by Eqs. 35 and 36 it still has the best output tracking response. The cost of this performance is high control activity, (Figure 12b).

Conclusion

A *hybrid* nonlinear control strategy associated with the structure of a *regular* perturbation system for the analysis and synthesis of the robust output regulation problem for a class of nonlinear systems with unmeasurable disturbances is presented. An illustrative example of CSTR is given to demonstrate the applicability of the proposed methods. Simulation results show that the proposed feedforward-like compensation with an admissible parameter by the simple parameter estimation is successfully applied to reject the single-input disturbance and multiinput disturbances problems. An important advantage of the proposed controller is that it can attenuate the effects of unmeasurable disturbances on the system output without using the conventional technique of high-gain feedback control. It can therefore avoid having active control actions and vigorous control moves in the control loop. The presented control method is suitable for process control.

Acknowledgment

The authors are grateful to an anonymous reviewer for his or her helpful comments on this work.

Notation

A = heat-transfer area
 C_{A_f} = reactant concentration in the feed
 $C_{A_{f0}}$ = base value of concentration in the feed
 C_{p_j} = heat capacity of cooling jacket
 C_{p_r} = heat capacity of reactor
 E = activation energy
 F_r = volumetric feed rate
 ΔH = heat of reaction
 k_0 = rate constant
 R = ideal gas constant
 T_r = reactor temperature
 T_{rf} = reactor temperature in the feed
 T_{rf0} = base value of temperature in the feed
 T_j = cooling jacket temperature
 U = heat-transfer coefficient
 V_r = reactor volume
 V_j = cooling jacket volume

Greek letters

α_i = adjustable parameters
 ξ, ξ_d, η = transformed state vector
 ρ_i = upper bounds
 l, γ = upper bounds
 ϵ = tuning parameter
 ρ_{or} = density of reactant
 ρ_{oj} = density of cooling jacket

Literature Cited

- Arkun, Y., and J.-P. Calvet, "Robust Stabilization of Input/Output Linearizable Systems under Uncertainty and Disturbances," *AIChE J.*, **38**, 1145 (1992).
 Callier, F., and C. Desoer, *Linear System Theory*, Springer-Verlag, New York (1991).
 Calvet, J.-P., and Y. Arkun, "Feedforward and Feedback Linearization of Nonlinear Systems and Its Implementation Using Internal Model Control (IMC)," *Ind. Eng. Chem. Res.*, **27**, 1822 (1988).
 Calvet, J.-P., and Y. Arkun, "Design of P and PI Stabilizing Controllers for Quasi-Linear Systems," *Comput. Chem. Eng.*, **14**, 415 (1990).
 Daoutidis, P., and C. Kravaris, "Synthesis of Feedforward/State Feedback Controller for Nonlinear Processes," *AIChE J.*, **35**, 1602 (1989).
 Henson, M. A., and D. E. Seborg, "Input-Output Linearization of General Nonlinear Processes," *AIChE J.*, **36**, 1753 (1990).
 Henson, M. A., and D. E. Seborg, "An Internal Model Control Strategy for Nonlinear Systems," *AIChE J.*, **37**, 1065 (1991).
 Isidori, A., *Nonlinear Control Systems*, 2nd ed., Springer-Verlag, New York (1989).
 Khalil, H. K., *Nonlinear Systems*, Macmillan, New York (1992).
 Khalil, H. K., and F. Esfandiari, "Semiglobal Stabilization of a Class of Nonlinear Systems Using Output Feedback," *IEEE Trans. Automat. Contr.*, **AC-38**, 1412 (1993).
 Kravaris, C., and C. B. Chung, "Nonlinear State Feedback Synthesis by Global Input/Output Linearization," *AIChE J.*, **34**, 592 (1987).
 Marino, R., W. Respondek, and A. I. van der Schaft, "Almost Disturbance Decoupling for Single-Input Single-Output Nonlinear Systems," *IEEE Trans. Automat. Contr.*, **AC-34**, 1013 (1989).
 Morari, M., and E. Zafiriou, *Robust Process Control*, Prentice-Hall, Englewood Cliffs, NJ (1989).
 Nijmeijer, H., and A. I. van der Schaft, *Nonlinear Dynamically Control Systems*, Springer-Verlag, New York (1990).
 Poslavsky, L., and J. Kantor, "Sliding Mode Control of an Exothermic Continuous Stirred Tank Reactor," *Proc. Amer. Contr. Conf.*, 2872 (1991).
 Shukla, N. V., P. B. Deshpande, V. R. Kumar, and B. D. Kulkarni, "Enhancing the Robustness of Internal-Model-Based Nonlinear pH Controller," *Chem. Eng. Sci.*, **48**, 913 (1993).

Sussmann, H. J., and P. V. Kokotovic, "The Peaking Phenomenon and Global Stabilization of Nonlinear Systems," *IEEE Trans. Automat. Contr.*, **AC-36**, 424 (1991).

Appendix

Proof of Theorem 1

To obtain the boundedness result, we define:

$$W(e, \eta) = W_1(e) + \mu W_0(\eta) \quad (A1)$$

with $W_1(e) = e^T P_s e$, where $W_0(\eta)$ is defined in Eq. 24 and μ is a strictly positive constant to be determined. Note that y_m and its r derivatives are bounded in Eq. 29. Thus, for a given bounded B_d , we obtain:

$$\|\xi\| \leq \|e\| + B_d. \quad (A2)$$

Differentiating $W(e, \eta)$ along the trajectory of the system in Eq. 43, we obtain:

$$\begin{aligned}
 \dot{W} \leq & -\|e\|^2 + \|e\| \sum_{i=1}^m |d_i(t) - p_i| \|2P_s \Delta A_i(x, p, u) \circ T^{-1}(\xi, \eta)\| \\
 & + \mu \left[\left\| \frac{\partial W_0}{\partial \eta} q(0, \eta) \right\| + \left\| \frac{\partial W_0}{\partial \eta} \right\| \|q(\xi, \eta) - q(0, \eta)\| \right. \\
 & \left. + \left\| \frac{\partial W_0}{\partial \eta} \right\| \sum_{i=1}^m |d_i(t) - p_i| \|\Delta \phi_i(x) \circ T^{-1}(\xi, \eta)\| \right]. \quad (A3)
 \end{aligned}$$

Under assumptions 2 and 4, this can be written as:

$$\begin{aligned}
 \dot{W} \leq & -\sum_{i=1}^m \left\{ \left[\frac{\|e\|}{2m} - \rho_i(\gamma_{1i} B_d + \gamma_{3i}) \right]^2 + \rho_i^2(\gamma_{1i} B_d + \gamma_{3i})^2 \right. \\
 & - \left(\frac{\|e\|}{2m} - \left[\mu k_4 \left(\frac{L}{m} + \rho_i l_{1i} \right) + \rho_i \gamma_{2i} \right] \|\eta\| \right)^2 \\
 & + \left[\mu k_4 \left(\frac{L}{m} + \rho_i l_{1i} \right) + \rho_i \gamma_{2i} \right]^2 \|\eta\|^2 \\
 & - \mu k_3 \left(\frac{\|\eta\|}{2m} - k_3^{-1} k_4 \left[B_d \left(\frac{L}{m} + \rho_i l_{1i} \right) + \rho_i l_{3i} \right] \right)^2 \\
 & + \mu k_3^{-1} k_4^2 \left[B_d \left(\frac{L}{m} + \rho_i l_{1i} \right) + \rho_i l_{3i} \right]^2 - \left(\frac{1}{2m} - \rho_i \gamma_{1i} \right) \|e\|^2 \\
 & - \frac{3}{4m} \mu k_3 \|\eta\|^2 + \mu k_4 \rho_i l_{2i} \|\eta\|^2 \Big\} \leq \sum_{i=1}^m \left\{ - \left(\frac{1}{2m} - \rho_i \gamma_{1i} \right) \|e\|^2 \right. \\
 & - \left(\frac{3}{4m} \mu k_3 - \left[\mu k_4 \left(\frac{L}{m} + \rho_i l_{1i} \right) + \rho_i \gamma_{2i} \right] - \mu k_4 \rho_i l_{2i} \right) \|\eta\|^2 \\
 & \left. + \rho_i^2(\gamma_{1i} B_d + \gamma_{3i})^2 + \mu k_3^{-1} k_4^2 \left[B_d \left(\frac{L}{m} + \rho_i l_{1i} \right) + \rho_i l_{3i} \right]^2 \right\}. \quad (A4)
 \end{aligned}$$

If we can define $l_{1_i}^* = (3k_3/8\rho_i k_4)$ and select $l_{2_i} \in (0, l_{1_i}^*)$ for every $i = 1, 2, \dots, m$, then we can set

$$l_{2_i}^* = \frac{1}{4m\gamma_{1_i}} \quad \text{and} \quad \mu_i^* = \frac{k_3}{8m \left[\rho_i \gamma_{2_i} + k_4 \left(\frac{L}{m} + \rho_i l_{1_i} \right) \right]^2} \quad (\text{A5})$$

for all $\mu \leq \max(\mu_1^*, \mu_2^*, \dots, \mu_m^*)$ and all $\rho_i \leq \min(\mu, l_{2_i}^*)$. So we have

$$\dot{W} \leq \sum_{i=1}^m \left\{ -\frac{\|e\|^2}{4m} - \frac{\mu k_3}{4m} \|\eta\|^2 + \rho_i^2 (\gamma_{1_i} B_d + \gamma_{3_i})^2 + \mu k_3^{-1} k_4^2 \left[B_d \left(\frac{L}{m} + \rho_i l_{1_i} \right) + \rho_i l_{3_i} \right]^2 \right\}. \quad (\text{A6})$$

Consequently, the states e and η are uniformly bounded for all $t \in [0, \infty]$. To investigate the ultimate bound of mismatch between the plant and the model in terms of ρ , we assume there exists a positive constant B_c such that $\|\eta\| \leq B_c$. Using $W_1(t)$, which is differentiated as

$$\begin{aligned} \dot{W}_1 &\leq -\|e\|^2 + \sum_{i=1}^m \rho_i^2 [\gamma_{1_i} (\|e\| + B_d) + \gamma_{2_i} \|\eta\| + \gamma_{3_i}] \\ &\leq \sum_{i=1}^m -\left(\frac{1}{m} - \frac{1}{4m} - \frac{1}{4m} - \rho_i \gamma_{1_i} \right) \|e\|^2 [\gamma_{1_i} (\|e\| + B_d) \\ &\quad + \gamma_{2_i} \|\eta\| + \gamma_{3_i}] \leq -\beta_1 W_1 + D_1, \end{aligned} \quad (\text{A7})$$

where $\beta_1 = 1/(4m\lambda_{\max}(P))$ and $D_1 = \sum_{i=1}^m \rho_i [(\gamma_{1_i} B_d + \gamma_{3_i})^2 + (\gamma_{2_i} B_c)^2]$. This implies that

$$W_1(t) \leq \left[W_1(0) - \frac{D_1}{\beta_1} \right] e^{-\beta_1 t} + \frac{D_1}{\beta_1}. \quad (\text{A8})$$

Consider the following inequality

$$\lambda_{\min}(P_s) \|e(t)\|^2 \leq W_1(t) \leq \lambda_{\max}(P_s) \|e(t)\|^2. \quad (\text{A9})$$

Then Eq. A8 can be reduced as the form of

$$\begin{aligned} \|e(t)\|^2 &\leq \left[\frac{\lambda_{\max}(P_s)}{\lambda_{\min}(P_s)} \|e(0)\|^2 - \frac{4m\lambda_{\max}(P_s)}{\lambda_{\min}(P_s)} D_2 \right] \\ &\quad \times \exp\left(-\frac{t}{4m\lambda_{\max}(P_s)} \right) + \frac{4m\lambda_{\max}(P_s)}{\lambda_{\min}(P_s)} D_2. \end{aligned} \quad (\text{A10})$$

If we select the initial condition, $\|e(0)\| \leq 2\sqrt{mD_2}$, we obtain

$$\|e(t)\| \leq \theta(\rho) = \sqrt{\frac{4m\lambda_{\max}(P_s)}{\lambda_{\min}(P_s)}} D_2, \quad \text{for } t \geq 0. \quad (\text{A11})$$

Thus the states are uniformly bounded in the size of the residual set, which is proportional to $\theta(\rho)$, with the property $\theta(0) = 0$, $\theta(\rho) > 0$, with $\rho \neq 0$. \square

Proof of Corollary 1

Equation A1 and the same algorithms that are described in the previous proof will be used. Differentiating $W(e, \eta)$ along the trajectory of the system in Eq. 53, and simplifying some terms, we obtain

$$\begin{aligned} \dot{W} &\leq -\left(\frac{1}{2} - \rho_i \gamma_{1_i} \right) \|e\|^2 - \left(\frac{3}{4} \mu k_3 [\mu k_4 (L + \rho_i l_{1_i}) + \rho_i \gamma_{2_i}]^2 \right. \\ &\quad \left. - \mu k_4 \rho_i l_{2_i} \right) \|\eta\|^2 + \rho_i^2 (\gamma_{1_i} B_d + \gamma_{3_i})^2 \\ &\quad + \mu k_3^{-1} k_4^2 [B_d (L + \rho_i l_{1_i}) + \rho_i l_{3_i}]^2. \end{aligned} \quad (\text{A12})$$

Next we can define

$$l_{1_i}^* = \frac{3k_3}{8\rho_i k_4}, \quad l_{2_i}^* = \frac{1}{4\gamma_{1_i}}, \quad \text{and} \quad \mu_i^* = \frac{k_3}{8[\rho_i \gamma_{2_i} + k_4 (L + \rho_i l_{1_i})]^2}.$$

After selecting $l_{2_i} \in (0, l_{1_i}^*)$ for all $\mu \leq \mu_i^*$ and all $\rho_i \leq \min(\mu, l_{2_i}^*)$, we obtain

$$\begin{aligned} \dot{W} &\leq -\frac{\|e\|^2}{4} - \frac{\mu k_3}{4} \|\eta\|^2 + \rho_i^2 (\gamma_{1_i} B_d + \gamma_{3_i})^2 \\ &\quad + \mu k_3^{-1} k_4^2 [B_d (L + \rho_i l_{1_i}) + \rho_i l_{3_i}]^2. \end{aligned} \quad (\text{A13})$$

Thus, states e and η are also uniformly bounded for all $t \in [0, \infty)$. Moreover, using $W_1(t)$, we obtain the boundedness

$$W_1(t) \leq \left[W_1(0) - \frac{D_i^0}{\beta^2} \right] e^{-\beta_2 t} + \frac{D_i^0}{\beta^2}, \quad (\text{A14})$$

where $\beta_2 = 1/(4\lambda_{\max}(P))$ and $D_i^0 = \rho_i^2 [(\gamma_{1_i} B_d + \gamma_{3_i})^2 + (\gamma_{2_i} B_c)^2]$. Therefore, we get

$$\|e(t)\| \leq \kappa_i \rho_i = \rho_i \sqrt{\frac{4\lambda_{\max}(P_s) [(\gamma_{1_i} B_d + \gamma_{3_i})^2 + (\gamma_{2_i} B_c)^2]}{\lambda_{\min}(P_s)}}, \quad \text{as } t \rightarrow \infty. \quad (\text{A15})$$

Thus the states are uniformly bounded in the size of the residual set, which is proportional to ρ_i , for $i = 1$ or $i = 2, \dots$, or $i = m$. \square

Proof of Corollary 2

Under the previous results for Corollary 1, the Schwartz inequality, and assumptions 2 and 5, we obtain

$$\begin{aligned} \dot{W} \leq & -\|e\|^2 + \rho^* \|e\| \sum_{i=1}^m [\gamma_1^* (\|e\| + B_d) + \gamma_2^* \|\eta\| + \gamma_3^*] \\ & + \mu \left\{ -k_3 \|\eta\|^2 + k_4 L (\|e\| + B_d) \|\eta\| \right. \\ & \left. + k_4 \rho^* \|\eta\| \sum_{i=1}^m [l_1^* (\|e\| + B_d) + l_2^* \|\eta\| + l_3^*] \right\}. \quad (A16) \end{aligned}$$

Then we can define

$$\begin{aligned} k_1^* &= \frac{3k_3}{8\rho^*k_4}, \quad k_2^* = \frac{1}{4\gamma_1^*}, \quad \text{and} \\ \mu_0^* &= \frac{k_3}{8[\rho^*\gamma_2^* + k_4(L + \rho^*l_1^*)]^2}. \end{aligned}$$

Under $l_2^* \in (0, k_1^*]$, for all $\mu \leq \mu_0^*$ and all $\rho^* \leq \min(\mu, k_2^*)$, we obtain

$$\begin{aligned} \dot{W} \leq & -\frac{\|e\|^2}{4} - \frac{\mu k_3}{4} \|\eta\|^2 + (\rho^*)^2 (\gamma_1^* B_d + \gamma_3^*)^2 \\ & + \mu k_3^{-1} k_4^2 [B_d(L + \rho^*l_1^*) + \rho^*l_3^*]^2. \quad (A17) \end{aligned}$$

Consequently, states e and η are also uniformly bounded for all $t \in [0, \infty)$. In the same way, we obtain the output tracking error

$$\begin{aligned} \|e(t)\|^2 \leq & \left[\frac{\lambda_{\max}(P_s)}{\lambda_{\min}(P_s)} \|e(0)\|^2 - \frac{4\lambda_{\max}(P_s)}{\lambda_{\min}(P_s)} \tilde{D}_0 \right] \\ & \times \exp\left(-\frac{t}{4\lambda_{\max}(P_s)}\right) + \frac{4\lambda_{\max}(P_s)}{\lambda_{\min}(P_s)} \tilde{D}_0, \quad (A18) \end{aligned}$$

where $\tilde{D}_0 = (\rho^*)^2 [(\gamma_1^* B_d + \gamma_3^*)^2 + (\gamma_2^* B_c)^2]$. Therefore, if $t \rightarrow \infty$, we obtain the results. \square

Proof of Proposition 1

Here we can direction calculate the derivatives of the output error as follows:

$$\begin{aligned} \dot{e}_1 &= L_{f_d} h - \dot{y}_m + \sum_{i=1}^m (d_i - p_i) L_{\omega_i} h \\ &= e_2 + \sum_{i=1}^m \vartheta_i(t) \Delta A_{i_1} \\ &\vdots \\ e_1^{(r-1)} &= L_{f_d}^{r-2} h - y_m^{(r-1)} + \sum_{i=1}^m \left\{ \sum_{j=1}^{r-1} [d_i(t) - p_i] \right. \\ &\quad \left. \times \frac{d^{r-i-1} L_{\omega_i} L_{f_d}^{j-1} h}{dt^{r-i-1}} + \frac{d^{r-i-1} [d_i(t) - p_i]}{dt^{r-i-1}} L_{\omega_i} L_{f_d}^{j-1} h \right\} \end{aligned}$$

$$\begin{aligned} &= e_r + \sum_{i=1}^m \left\{ \sum_{j=1}^{r-1} \left[\vartheta_i(t) \frac{d^{r-i-1} \Delta A_{i_j}}{dt^{r-i-1}} + \frac{d^{r-i-1} \vartheta_i(t)}{dt^{r-i-1}} \Delta A_{i_j} \right] \right\} \\ e_1^{(r)} &= \dot{e}_r + \sum_{i=1}^m \left\{ \sum_{j=1}^r [d_i(t) - p_i] \frac{d^{r-i} L_{\omega_i} L_{f_d}^{j-1} h}{dt^{r-i}} \right. \\ &\quad \left. + [d_i(t) - p_i]^{(r-i)} L_{\omega_i} L_{f_d}^{j-1} h \right\} \\ &= -\alpha_1 e_1 - \dots - \alpha_r e_r + \sum_{i=1}^m \left\{ \sum_{j=1}^r \right. \\ &\quad \left. \times \left[\vartheta_i(t) \frac{d^{r-i} \Delta A_{i_j}}{dt^{r-i}} + \vartheta_i^{(r-i)}(t) \Delta A_{i_j} \right] \right\} \\ &= -\alpha_1 e_1 - \dots - \alpha_r \left\{ e_1^{(r-1)} - \sum_{i=1}^m \right. \\ &\quad \left. \times \left[\sum_{j=1}^{r-1} \left(\vartheta_i(t) \frac{d^{r-i-1} \Delta A_{i_j}}{dt^{r-i-1}} + \vartheta_i^{(r-i-1)}(t) \Delta A_{i_j} \right) \right] \right\} \\ &\quad + \sum_{i=1}^m \left[\sum_{j=1}^r \left(\vartheta_i \frac{d^{r-i} \Delta A_{i_j}}{dt^{r-i}} + \vartheta_i^{(r-i)}(t) \Delta A_{i_j} \right) \right]. \quad (A19) \end{aligned}$$

This completes the proof. \square

Proof of Proposition 2

From the result of Barbalat's lemma (Khalil, 1992), if Eq. 62 exists and i is finite, then $|e_i(t)| \leq \tilde{\epsilon}$ as $t \rightarrow nt_1$ (sufficiently large n), where $\tilde{\epsilon} (\tilde{\epsilon} \geq 0)$ is a sufficiently small value. After a period of time, that is, $t \rightarrow nt_1$, the time derivatives of $e_1^{(j)}$ and $\vartheta^{(j)}$ will approach sufficiently small values. Then Eq. 63 can be written as:

$$\begin{aligned} \lim_{t \rightarrow nt_c} \alpha_1 e_1 &= \lim_{t \rightarrow nt_c} \sum_{i=1}^r \left\{ \sum_{j=1}^r [\vartheta_i(t) \Delta A_{i_j}^{(r-j)}(x, p, u)] \right. \\ &\quad \left. + \sum_{j=1}^r \alpha_j \sum_{k=1}^j [\vartheta_i(t) \Delta A_{i_k}^{(j-k)}(x, p, u)] \right\}. \quad (A20) \end{aligned}$$

Moreover, choosing $m = 1$, yields:

$$\begin{aligned} \lim_{t \rightarrow nt_c} \alpha_1 e_1 &= \lim_{t \rightarrow nt_c} \vartheta_1(t) \left\{ \sum_{j=1}^r [\Delta A_{i_j}^{(r-j)}(x, p, u)] \right. \\ &\quad \left. + \sum_{j=1}^r \alpha_j \sum_{k=1}^j [\Delta A_{i_k}^{(j-k)}(x, p, u)] \right\}. \quad (A21) \end{aligned}$$

Obviously, when the signal $|e_1|$ is below a sufficiently small value, the parameter p_i will converge to a fixed value, for $i = 1$ or $i = 2, \dots$, or $i = m$. \square

Manuscript received July 22, 1994, and revision received Nov. 22, 1994.